ALTERRA.
Wageningen Universiteit & Research centre
Omgevingswetenschappen
Centrum Water & Klimaat
Team Integraal Waterbeheer

ICW note 1713
June 1986

nota

instituut voor cultuurtechniek en waterhuishouding, wageningen

FORMULATION OF A MODEL DESCRIBING THE WEATHERING PROCESS OF $CaCO_3$ IN SOILS

drs. C.J. Ritsema

C O N T E N T S

ALTERRA,
Wageningen Universiteit & Research centre
Omgevingswetenschappen
Centrum Water & Klimaat
Team Integraal Waterbeheer

1. INTRODUCTION

One of the conclusions of ICW-nota 1682 (RITSEMA, 1985) is that dissolution, c.q. weathering, of minerals can be written as:

$$J = Kt \,.\, (Cg-Cb) = Kc \,.\, (Cs-Cg)^n \qquad (1)$$

where: J = mass flux of species C (mole/cm^2.s)
Kt = diffusion velocity of species C (cm/s)
Cg = concentration of species C in the diffuse boundary layer near the solid phase (mole/ml)
Cb = concentration of species C in the soil solution (mole/ml)
Kc = chemical velocity constant C(if n=1 Kc has the dimension cm/s, if n=2 cm.ml/mole.s)
Cs = concentration of species C at the solid surface (mole/ml)
n = a dimensionless exponent

The value of n is variabel and depends on the specific mineral and the prevailing pH. STUMM and MORGAN (1970) give n-values for potassium chloride (n=1), magnesium oxalate (n=2), silver chloride (n=2) and silver chromate (n=3). The n-values cited in literature for $CaCO_3$ vary from author to author. For example, according to WIECHERS et al (1975), SJOBERG and RICKARD (1984) and MORETO et al (1984) n=1. These authors are considering the ion product $[Ca^{++}].[CO_3^{2-}]$ in their investigations and not the Ca^{++} concentration alone.

When taking into account only the Ca^{++} concentration, according to NANCOLLAS and REDDY (1971), PLUMMER et al (1976, 1978) and REDDY (1978), n will have the value 2. According to PLUMMER et al (1976) this value is valid till a pH-value of 5.94. Above this lower pH region n will receive the value 4 (see Fig. 1).

Recent investigations carried out by GOBRAN and MIYAMOTO (1985), however, show that the solution of $CaCO_3$ up to a pH value of 7 can be described by equation 1 with n=2.

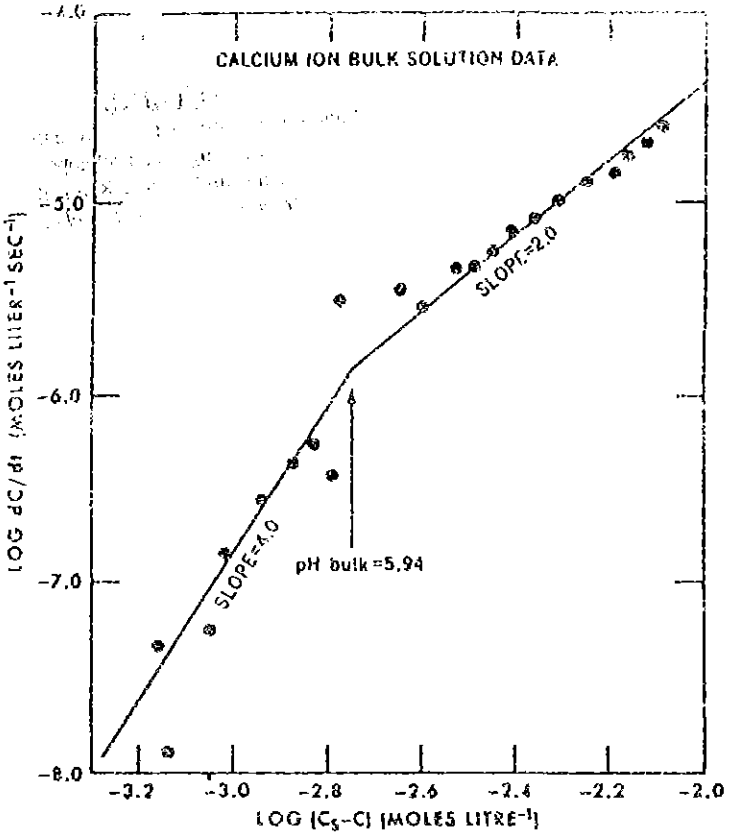

Fig. 1. Log rate of change of concentration versus log saturation deficit in the bulk solution for calcium ion. Beyond pH 5.94 there is a change from a second order to a fourth order process (after PLUMMER et al, 1978)

In this paper equation 1 will be elaborated for the n-values 1, 2 and 4. Next the variables necessary to quantify the $CaCO_3$ weathering process are formulated. Finally a model is presented with which it is possible to simulate the weathering of $CaCO_3$ in dependance of the pH, HCO_3^- concentration, flow velocity etc. The model describes one dimensional flow, ignores adsorption, and is based on the mixing-cell concept.

2. THEORETICAL BACKGROUND

2.1. First order dissolution processes

If n=1 it follows that relation 1 can be written as:

$$Ce \cdot Kt \cdot \left(\frac{Cg}{Ce} - \frac{Cb}{Ce}\right) = Kc \cdot Cs \cdot \left(\frac{Cs}{Cs} - \frac{Cg}{Cs}\right) \qquad (2)$$

Assuming that the concentration of the chemical component at the solid surface, Cs, equals the (theoretical) equilibrium concentration of the bulk solution, Ce, it follows that:

$$Ce \cdot Kt \cdot \left(\frac{Cg}{Ce} - \frac{Cb}{Ce}\right) = Kc \cdot Ce \cdot \left(1 - \frac{Cg}{Ce}\right) \qquad (3)$$

Supposing

$$X = \frac{Cb}{Ce} \quad \text{and} \quad Y = \frac{Cg}{Ce} \qquad (4)$$

equation 3 can be written as:

$$Ce \cdot Kt \cdot (Y-X) = Kc \cdot Ce \cdot (1-Y) \qquad (5)$$

or

$$\frac{Kt}{Kc} \cdot (Y-X) = (1-Y) \qquad (6)$$

X and Y are dimensionless analogs of respectively the bulk solution and surface boundary layer concentrations.
If

$$P = \frac{Kt}{Kc} \qquad (7)$$

it follows that equation 1, with the introduction of the dimensionless parameters X, Y and P, can be written as:

$$(1-Y) = P \cdot (Y-X) \qquad (8)$$

or

$$Y = \frac{1 + PX}{1 + P} \qquad (9)$$

The time which is necessary to reach a certain degree of saturation of the bulk solution can be calculated supposing no inhibition is taking place.

Combination of equation 1 and

$$J = \frac{V}{A} \cdot \frac{dCb}{dt} \qquad (10)$$

results in:

$$\frac{V}{A} \cdot \frac{dCb}{dt} = Kt \cdot (Cg-Cb) \qquad (11)$$

where: V = volume of soil water (cm^3)
A = soil mineral surface (cm^2)

Dividing equation 11 by Ce results in:

$$\frac{dCb/Ce}{dt} = \frac{A.Kt}{V} \cdot \left(\frac{Cg}{Ce} - \frac{Cb}{Ce}\right) \qquad (12)$$

or

$$\frac{dX}{dt} = \frac{A.Yt}{V} \cdot (Y-X) \qquad (13)$$

When assuming that

$$Ts = \frac{V}{A.Kt} \qquad (14)$$

it follows that equation 13 also can be written as:

$$\frac{dX}{dt} = \frac{1}{Ts} \cdot (Y-X) \qquad (15)$$

Substitution of equation 9 in equation 15 results in:

$$\frac{dX}{dt} = \frac{1}{Ts} \cdot \left(\frac{1+PX}{1+P} - X\right) \qquad (16)$$

or

$$\frac{dX}{(1-X)} = \frac{dt}{(1+P) \cdot Ts} \qquad (17)$$

Integration of this equation results into:

$$- \ln(1-X) = \frac{1}{(1+P) \cdot Ts} \cdot t + c \qquad (18)$$

For t=0 is X=0 and thus c=0.
Equation 18 can also be written as:

$$X = 1 - e^{- \frac{t}{(1+P) \cdot Ts}} \qquad (19)$$

The general solution of equation 15 consists of a range of curves depending on the values of P and Ts. For one soil type Ts can be considered as a constant. If P reaches very low values the solution converges to equation 20:

$$X = 1 - e^{-t/Ts} \qquad (20)$$

If P reaches very high values the solution of equation 17 approaches the equation:

$$X = 1 - e^{-0} = 0 \qquad (21)$$

Fig. 2 shows a graphical representation of equation 19 for P=0.

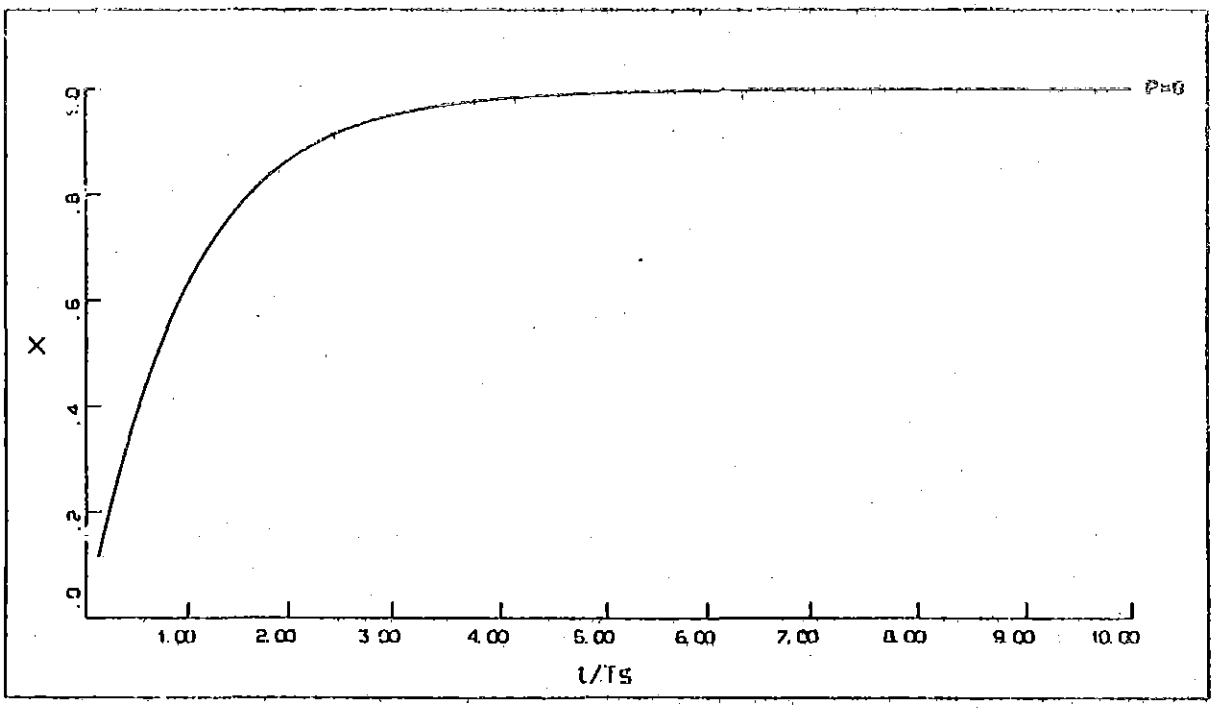

Fig. 2. f(X, t/Ts) for n=1 and P=0

2.2. Second order dissolution processes

If n=2 equation 1 can be written as:

$$Ce \cdot Kt \cdot \left(\frac{Cg}{Ce} - \frac{Cb}{Ce}\right) = Cs^2 \cdot Kc \cdot \left(\frac{Cs}{Cs} - \frac{Cg}{Cs}\right)^2 \qquad (22)$$

and assuming Cs = Ce it follows that:

$$Ce \cdot Kt \cdot (Y-X) = Ce^2 \cdot Kc \cdot (1-Y)^2 \qquad (23)$$

or

$$\frac{Kt}{Ce \cdot Kc} \cdot (Y-X) = (1-Y)^2$$

Supposing

$$P_{n=2} = \frac{Kt}{Ce \cdot Kc} \qquad (24)$$

it follows that

$$P_2 \cdot (Y-X) = (1-Y)^2 \qquad (25)$$

Expressing Y in X and P_2 results in:

$$Y = 1 + \frac{1}{2}\left[P_2 - \sqrt{(P_2^2+4P_2(1-X))}\right] \tag{26}$$

Only the solution with the negative square root is correct because Y can only have a value between 0 and 1.

In this case it is also possible to calculate the degree of saturation of the bulk solution with help of the equation:

$$\frac{dX}{dt} = \frac{1}{Ts} \cdot (Y-X) \tag{27}$$

Substitution of equation 26 in equation 27 gives the complete differential equation for the case with n=2. Integrating, expressing X implicit in t, results in:

$$\ln\left\{\frac{f(P_2,X)}{f(P_2,0)}\right\} - P_2 \cdot \left\{\frac{1}{f(P_2,X)} - \frac{1}{f(P_2,0)}\right\} = -\frac{t}{2.Ts} \tag{28}$$

where:

$$f(P_2,X) = \sqrt{(P_2^2+4P_2(1-X))} - P_2 \tag{29}$$

and where $f(P_2,0)$ is the value of $f(P_2,X)$ for $X = 0$.

Equation 28 represents the complete solution of equation 1 in the case with n=2. If Ts is a constant for a certain soil type equation 28 consists of a range of curves in dependance of P_2

For very low values of P_2 the solution can be written as:

$$1 - X = e^{-t/Ts} \tag{30}$$

If the value of P_2 is very high the solution converges to

$$\frac{X}{1 - X} = \frac{t}{P_2.Ts} \tag{31}$$

or

$$X = \frac{t}{t + P_2.Ts} \tag{32}$$

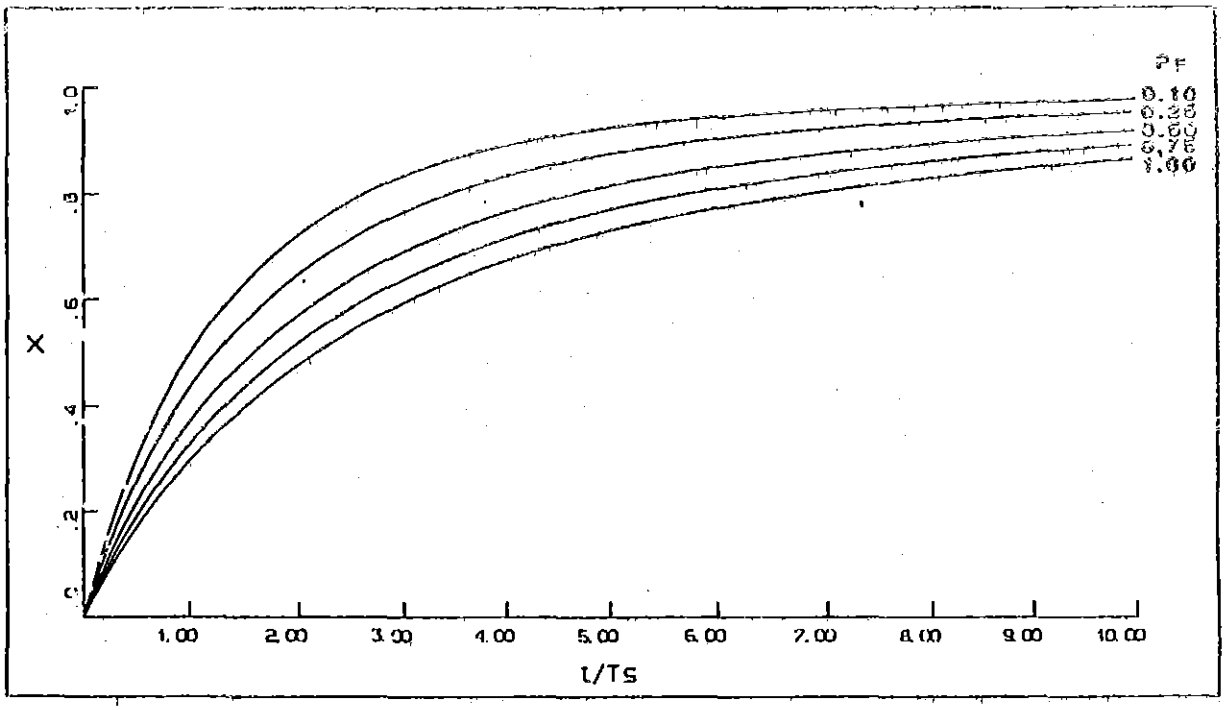

Fig. 3. f(X,t/Ts) for different P_2 values with n=2

In the case the value of P_2 exceeds the value of t many times equarion 32 will approach 0.

In Fig. 3 a graphical representation of X against t/Ts is given for different P_2-values

2,3. Fourth order dissolution processes

In the case n=4 equation I can be written as:

$$Ce \cdot Kt \cdot \left(\frac{Cg}{Ce} - \frac{Cb}{Ce}\right) = Cs^4 \cdot Kc \cdot \left(\frac{Cs}{Cs} - \frac{Cg}{Cs}\right)^4 \qquad (33)$$

Assuming Cs = Ce it follows that

$$Ce \cdot Kt \cdot (Y-X) = Ce^4 \cdot Kc \cdot (1-Y)^4 \qquad (34)$$

or

$$\frac{Kt}{Ce^3 . Kc} \cdot (Y-X) = (1-Y)^4$$

Supposing

$$P_{n=4} = \frac{Kt}{Ce^3.Kc} \tag{35}$$

it follows that

$$P_4 \cdot (Y-X) = (1-Y)^4 \tag{36}$$

or

$$Y^4 - 4Y^3 + 6Y^2 + Y(-4-P_4) + 1 + P_4X = 0 \tag{37}$$

This is an equation of the form:

$$Y^4 + a_1Y^3 + a_2Y^2 + a_3Y + a_4 = 0 \tag{38}$$

The only, real, solution of this equation appears to be:

$$Y = \frac{-b \cdot \sqrt{b^2 - 4ac}}{2a} \tag{39}$$

where: a = 1

$$b = \frac{1}{2}\{a_1 - \sqrt{a_1^2 - 4a_2 + 4Z}\}$$

$$c = \frac{1}{2}\{Z - \sqrt{Z^2 - 4a_4}\}$$

and

$$Z = \sqrt[3]{8P_4(1+X) + \frac{1}{2}P_4^2 + \sqrt{(-\frac{4}{9}P_4(1+X))^3 + (8P_4(1+X) + \frac{1}{2}P_4^2)^2}} +$$

$$+ \sqrt[3]{8P_4(1+X) + \frac{1}{2}P_4^2 - \sqrt{(-\frac{4}{9}P_4(1+X))^3 + (8P_4(1+X) + \frac{1}{2}P_4^2)^2}} + 2$$

Besides equation 39 equation 15 is also valid. This equation can be written as:

$$\frac{dX}{d(t/Ts)} = (Y-X) \tag{40}$$

Which leaves a system of two equations with 4 unknown variables (X, Y, P_4 and t/Ts). With help of the computer X and Y have been calculated in the t/Ts-range from 0 up till 10 for different values of P_4.

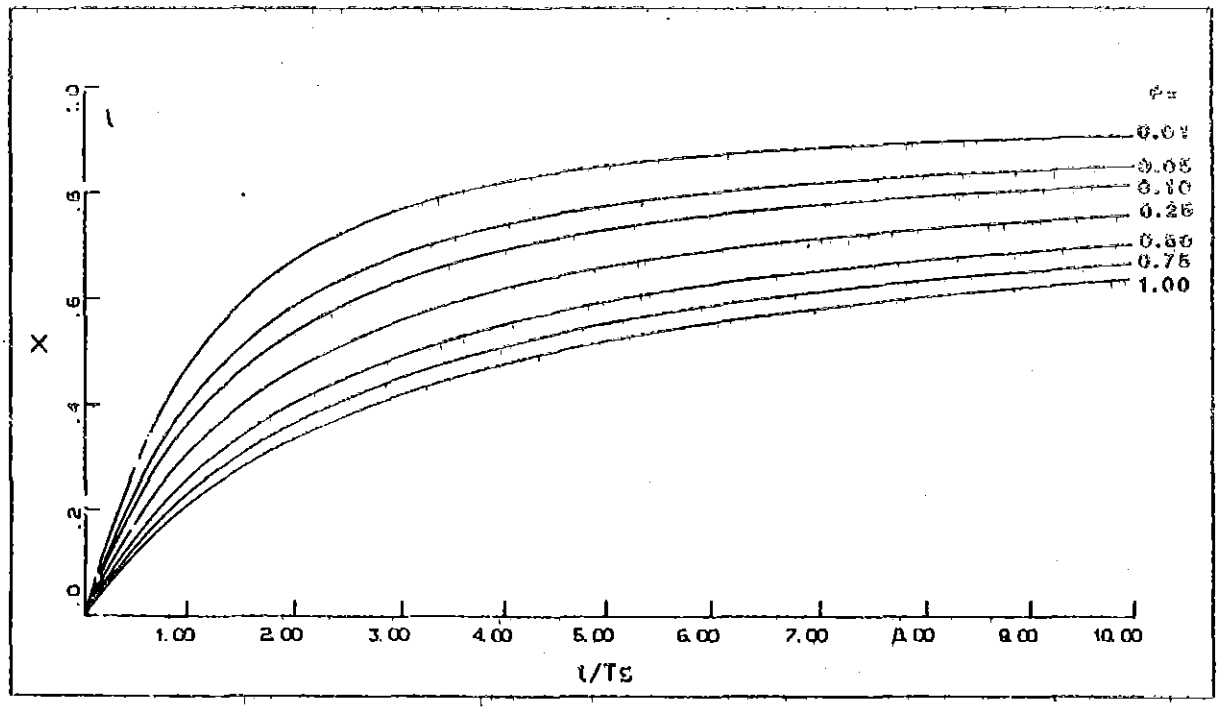

Fig. 4. f(X,t/Ts) for different P_4 values with n=4

Furthermore a graphical representation of X against t/Ts is given for different values of P_4 (see Fig. 4).

3. THE DISSOLUTION OF $CaCO_3$

3.1. Definition of Ce

The theoretical solutions in the case n=1, 2 or 4 are all functions of X against t/Ts (and P).

X equals Cb/Ce and is thus a variable expressing the degree of saturation of the bulk solution, If there is no Ca^{++} in solution X has the value 0; when X=1 the bulk solution is completely saturated with respect to Ca^{2+}. In the case of pure equilibrium between $CaCO_3$ and the liquid phase it follows that:

$$CaCO_3 \rightleftharpoons Ca^{2+} + CO_3^{2-} \qquad (41)$$

The solubility product can be written as:

$$K_{so} = [Ca^{2+}] \cdot [CO_3^{2-}] \qquad (42)$$

and thus

$$[Ca^{2+}] = \frac{K_{so}}{[CO_3^{2-}]} = Ce \qquad (43)$$

The degree of saturation of the bulk solution of the soil system cannot be described in this manner. If one supposes that the increase in the time of the Ca^{2+} concentration in the bulk solution is the result of the weathering of calcite ($CaCO_3$) and that this also influences the possible changes in the HCO_3^- concentration it follows, according to STUMM and MORGAN (1970), BOLT and BRUGGENWERT (1976) and KEMMERS (1985), that

$$\log[Ca^{2+}] + \log[HCO_3^-] - \log[H^+] = 1.98 \qquad (44)$$

and thus

$$[Ca^{++}] = \frac{10^{1.98-pH}}{[HCO_3^-]} = Ce \qquad (45)$$

In the case n=1 equation 19 can also be written as:

$$\frac{Cb}{Ce} = 1 - e^{-\frac{t}{(1+P).Ts}}$$

Combination with equation 45 results into:

$$[Ca^{++}] = \frac{10^{1.98-pH}}{[HCO_3^-]} \cdot \left(1-e^{-\frac{t}{(1+P).Ts}}\right) \qquad (46)$$

Also in the case n=2 or 4 it is possible to substitute equation 45 in the theoretical equation concerned.

3.7. Definition of P

Wheather n=1, 2 or 4, in either case the value of P is dependent on the ratio between Kt and Kc and eventually Ce (see equations 7, 24 and 35). How Ce can be defined has already be shown aboye.

First of all the definition of Kt will be discussed. According to RITSEMA (1985) the diffusion velocity and the diffusion coefficient are related to each other as follows:

$$Kt = \frac{D}{dg} \qquad (47)$$

where

Kt = diffusion velocity (cm/s)
D = diffusion coefficient for Ca^{2+}-ions (cm^2/s)
dg = thickness of the diffuse boundary layer (cm)

The diffusion coefficient D is dependent on the temperature. SJOBERG and RICKARD (1984) give temperature and D values for the $CaCO_3$-dissolution process (see Table 1).

The difficulty in equation 47 is defining the thickness of the diffuse boundary layer dg. This thickness is dependent on the flow velocity of the bulk solution. Assuming that soil grains can be considered as very small flat circular plates it follows, according to PLESKOV and FILINOVSKI (1976), that

$$dg = \frac{1.61 . D^{1/3} . \nu^{1/6}}{\omega^{1/2}} \qquad (48)$$

Table 1. Temperature diffusion coefficient values according to SJOBERG and RICKARD (1984)

Temperature (^oC)	Diffusion coefficient ($* 10^{-6}$ cm^2/s)
1	1.66
10	3.49
14	4.71
18	5.82

where: ν = kinematic viscosity (cm^2/s)

ω = rotational velocity (1/s)

The average flow velocity of the bulk solution, $\bar{V}$, can be described as:

$$\bar{V} = \frac{3}{4} \cdot 2\pi\bar{r} \cdot \omega \qquad (49)$$

where: $\bar{V}$ = average flow velocity of the bulk solution (cm/s)

$\bar{r}$ = average radius of the $CaCO_3$-grains (cm)

By substituting equation 49 into equation 48 it is possible to eliminate the rotational velocity ω. The result is:

$$dg = \frac{1.61 . D^{1/3} . \nu^{1/6} . (3\pi\bar{r})^{1/2}}{2(\bar{V})^{1/2}} \qquad (50)$$

An increase in the flow velocity consequently causes a decrease in the thickness of the diffuse boundary layer. Combination of equation 50 and 47 results in:

$$Kt = \frac{D . (2\bar{V})^{1/2}}{1.61 . D^{1/3} . \nu^{1/6} . (3\pi\bar{r})^{1/2}} \qquad (51)$$

Assuming that $\bar{r}$ = 50 µm and the temperature equals 10^oC (and thus $D = 3.49.10^{-6}$ cm^2/s and $\nu = 1.31.10^{-2}$ cm^2/s) it follows that:

$$Kt = 18.7.10^{-4} . (\bar{V})^{1/2} \qquad (52)$$

In order to quantify the value of P in a certain case it is necessary to know the value of Kc besides the value of the average flow velocity.

PLUMMER and WIGLEY (1976) and SJOBERG and RICKARD (1984) give different Kc-values in the case n=1, 2 and 4, as can be seen in Table 2.

Substituting these Kc-values and equation 52 in respectively equation 7, 24 and 35 results in different formulations for P in the case n=1, 2 and 4 (see Table 3).

Table 2. Different values of Kc in dependence of n

n=1	$Kc = 6.5.10^{-3}$ cm/s	SJOBERG and RICKARD (1984), page 483
n=2	$Kc = 3.1.10^{-2}$ cm.l/mole.s	PLUMMER and WIGLEY (1976), page 199
n=4	$Kc = 1.4.10^{4}$ cm.l^3/$mole^3$.s	PLUMMER and WIGLEY (1976), page 196

Table 3. Formulations for P in the case n=1, 2 and 4

n=1	$P = 2.9.10^{-1} \ (\bar{V})^{1/2}$
n=2	$P = 6.0.10^{-2} \ (\bar{V})^{1/2}/Ce$
n=4	$P = 1.3.10^{-7} \ (\bar{V})^{1/2}/Ce^3$

3.3. Definition of Ts

Ts can be described as:

$$Ts = \frac{V}{A} \cdot \frac{1}{Kt} \qquad (53)$$

where: V = moisture content (cm^3/cm^3)
A = soil mineral surface (cm^2/cm^3)
Kt = diffusion velocity (cm/s)

When the porosity of the soil and the flow velocity of the percolating water are known it is possible to calculate V and Kt.

The variable A is dependent on the soil type but will most probably exhibit considerable spatial variability within such a soil unit. In hydrological studies it is uncommon to determine soil mineralogy with a sufficient accuracy to quantify the factor A. The consequence is that the value of Ts is unknown in most of the hydrological surveys. However, the value of Ts can be calculated afterwards when concentration depth field data are being compared with theoretical X-t/Ts relations. This is possible because each depth is related to a certain residence time of the water. By changing the Ts-value one finds one theoretical concentration time relation that will correspond to the concentration depth field data. If this is the case the $CaCO_3$-weathering model is validated and simulation calculations can be carried out.

4. MODEL DESCRIPTION

The model is based on the continuity equation and describes one-dimensional stationary flow.

In mathematical formulation this leads to:

$$\varepsilon \cdot \Delta x \cdot \frac{dCb}{dt} = q \cdot C_{i-1} - q \cdot C_i + \varepsilon \cdot \Delta x \cdot \left(\frac{dCb}{dt}\right)_w \qquad (54)$$

where: ε = porosity (dimensionless)
Δx = thickness of the soil layer (m)
Cb = Ca^{2+} concentration in the bulk solution (mole/l)
q = flux (m/s)
C_{i-1} = Ca^{2+} concentration of the inflowing water (mole/l)
C_i = Ca^{2+} concentration of the outflowing water (mole/l)
$\left(\frac{dCb}{dt}\right)_w$ = increase in Ca^{2+} concentration as a result of the $CaCO_3$-weathering

The last term of equation 54, i.e. the Ca^{2+} production term as result of the $CaCO_3$-weathering, can be rewritten. Equation 15 can be written as:

$$\left(\frac{dCb}{dt}\right)_w = \frac{Ce}{Ts}\left(Y - \frac{Cb}{Ce}\right) \qquad (55)$$

Assuming n=2 and substituting equation 26 in equation 55 gives

$$\left(\frac{dCb}{dt}\right)_w = \frac{Ce}{Ts} \cdot \left\{\left(1 + \frac{1}{2}P_2 - \frac{1}{2}\sqrt{P_2^2 + 4P_2\left(1 - \frac{Cb}{Ce}\right)}\right) - \frac{Cb}{Ce}\right\} \qquad (56)$$

or

$$\left(\frac{dCb}{dt}\right)_w = \frac{1}{Ts} \cdot \left\{Ce + \frac{1}{2}P_2 \cdot Ce - \frac{1}{2}Ce\sqrt{P_2^2 + 4P_2\left(1 - \frac{Cb}{Ce}\right)} - Cb\right\} \qquad (57)$$

Substituting equation 57 in the continuity equation gives:

$$\varepsilon \cdot \Delta x \cdot \frac{dC_i}{dt} = q \cdot C_{i-1} - q \cdot C_i +$$

$$+ \varepsilon \cdot \Delta x \cdot \left\{\frac{1}{Ts}\left(Ce + \frac{1}{2}P_2 \cdot Ce - \frac{1}{2}Ce\sqrt{P_2^2 + 4P_2\left(1 - \frac{C_i}{Ce}\right)} - C_i\right)\right\} \qquad (58)$$

The simulation calculations are based on (BLÖMEN, 1985; GROENENDIJK, 1985; VAN OMMEN, 1985):

$$\frac{dC_i}{dt} = \frac{C_{i,j+1} - C_{i,j}}{\Delta t} \qquad (59)$$

where: $C_{i,j}$ = initial Ca^{2+} concentration in soil layer i at time j
$C_{i,j+1}$ = the Ca^{2+} concentration in soil layer i at time j+1

Substituting equation 59 in equation 58 gives:

$$C_{i,j+1} = C_{i,j} + \frac{t}{\varepsilon.\Delta x} \cdot \{q.C_{i-1,j} - q.C_{i,j}\} +$$

$$+ \frac{\Delta t}{Ts} \cdot \{Ce + \frac{1}{2} P_2 . Ce - \frac{1}{2} Ce . \sqrt{P_2^2 + 4P_2(1 - \frac{C_{i,j}}{Ce})} - C_{i,j}\} \qquad (60)$$

As a rough approach the first calculations can be carried out with constant pH, HCO_3^- concentration (and thus constant Ce) and P value.

In the simulation $C_{i,j+1}$ will be calculated for every soil layer with thickness Δx, at each timestep Δt. After the Ca^{2+} concentrations in the whole profile (soil column) have been calculated for the first timestep the calculation starts again at the top of the soil column for timestep 2 etc. The calculations will continue until a (dynamic) steady-state concentration-depth profile has been established throughout the whole soil column. The calculated steady-state situation is the result of the interaction between the chemical rate constant Kc (i.e. the degree into which a mineral can be weathered/dissolved), the hydrological circumstances (i.e. the degree in which a component can be transported) and the specific soil conditions (Ts, pH, HCO_3^- temperature etc.).

This type of calculations can be carried out for different hydrological circumstances and soil conditions.

5. SENSITIVITY ANALYSIS

For a better understanding of the weathering process of $CaCO_3$ a series of graphics is constructed in which the influence of the different variables involved is being shown. The various graphics are:

Fig. 5 until 7 Influence of Ts
Fig. 8 until 10 Influence of the flux q
Fig. 11 until 13 Influence of Ca^{2+}-feed
Fig. 14 until 16 Influence of Ca^{2+}-initial
Fig. 17 until 19 Influence of pH

The data used in the calculations are shown in Table 4.

Figures 5 until 7 show the influence of the quantity of solid $CaCO_3$ in the soil on the Ca^{++} saturation degree with increasing depth. The Ca^{++} saturation concentration can be considered as a constant following equation 45. With help of the equations 52 and 53 it is possible to calculate the value of factor A. The Fig. 5, 6 and 7 are related to respectively an A-factor of 6.5, 13 and 65 cm^2 solid $CaCO_3/cm^3$ soil.

Table 4. Data used in the sensitivity analysis

Figure No.	Ts (s)	Por. (-)	Flux (m/day)	Ca^{2+} feed (mole/l)	Ca^{2+} initial (mole/l)	pH (-)	HCO_3^- (mole/l)	Ca^{2+} satur. =Ce (mole/l)
5	10,000	0.3	0.004	0.0	0.0	6.0	0.0013	0.0735
6	5,000	0.3	0.004	0.0	0.0	6.0	0.0013	0.0735
7	1,000	0.3	0.004	0.0	0.0	6.0	0.0013	0.0735
8	10,000	0.3	0.004	0.0	0.0	6.0	0.0013	0.0735
9	10,000	0.3	0.002	0.0	0.0	6.0	0.0013	0.0735
10	10,000	0.3	0.0004	0.0	0.0	6.0	0.0013	0.0735
11	10,000	0.3	0.004	0.024	0.048	6.0	0.0013	0.0955
12	10,000	0.3	0.004	0.048	0.048	6.0	0.0013	0.0955
13	10,000	0.3	0.004	0.072	0.048	6.0	0.0013	0.0955
14	10,000	0.3	0.004	0.0002	0.024	6.0	0.0013	0.0735
15	10,000	0.3	0.004	0.0002	0.048	6.0	0.0013	0.0735
16	10,000	0.3	0.004	0.0002	0.072	6.0	0.0013	0.0735
17	5,000	0.3	0.004	0.04	0.070	6.0	0.0013	0.0735
18	5,000	0.3	0.004	0.04	0.070	5.5	0.0013	0.2323
19	5,000	0.3	0.004	0.04	0.070	5.0	0.0013	0.7346

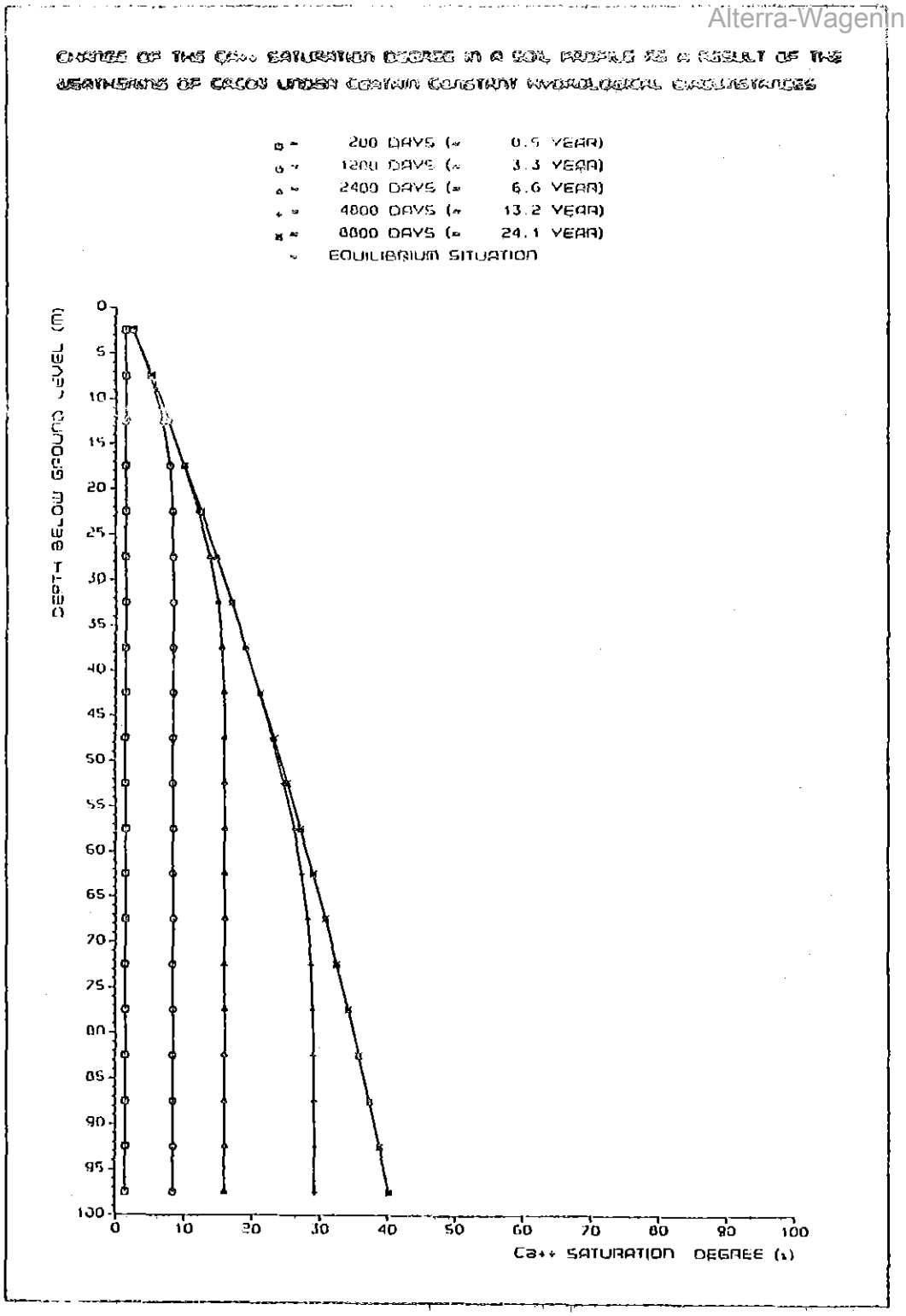

Fig. 5. Influence of Ts on the realization of the Ca^{++} saturation degree-depth profile. Ts = 10,000 s. The values of the other parameters are equal to the values use in the Fig. 6 and 7

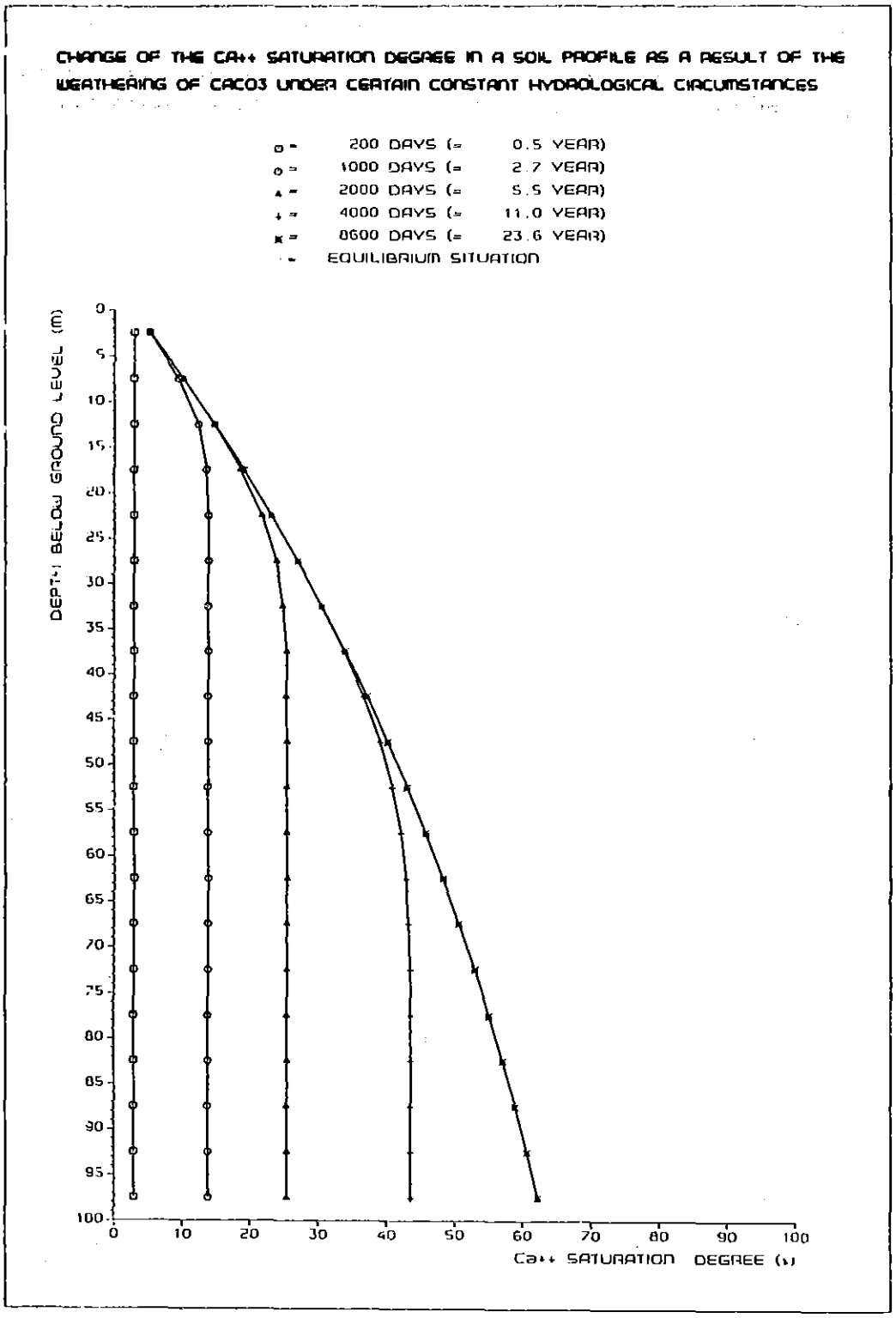

Fig. 6. Influence of Ts on the realization of the Ca^{++} saturation degree-depth profile. Ts = 5,000 s. The values of the other parameters are equal to the values used in the Fig. 5 and 7

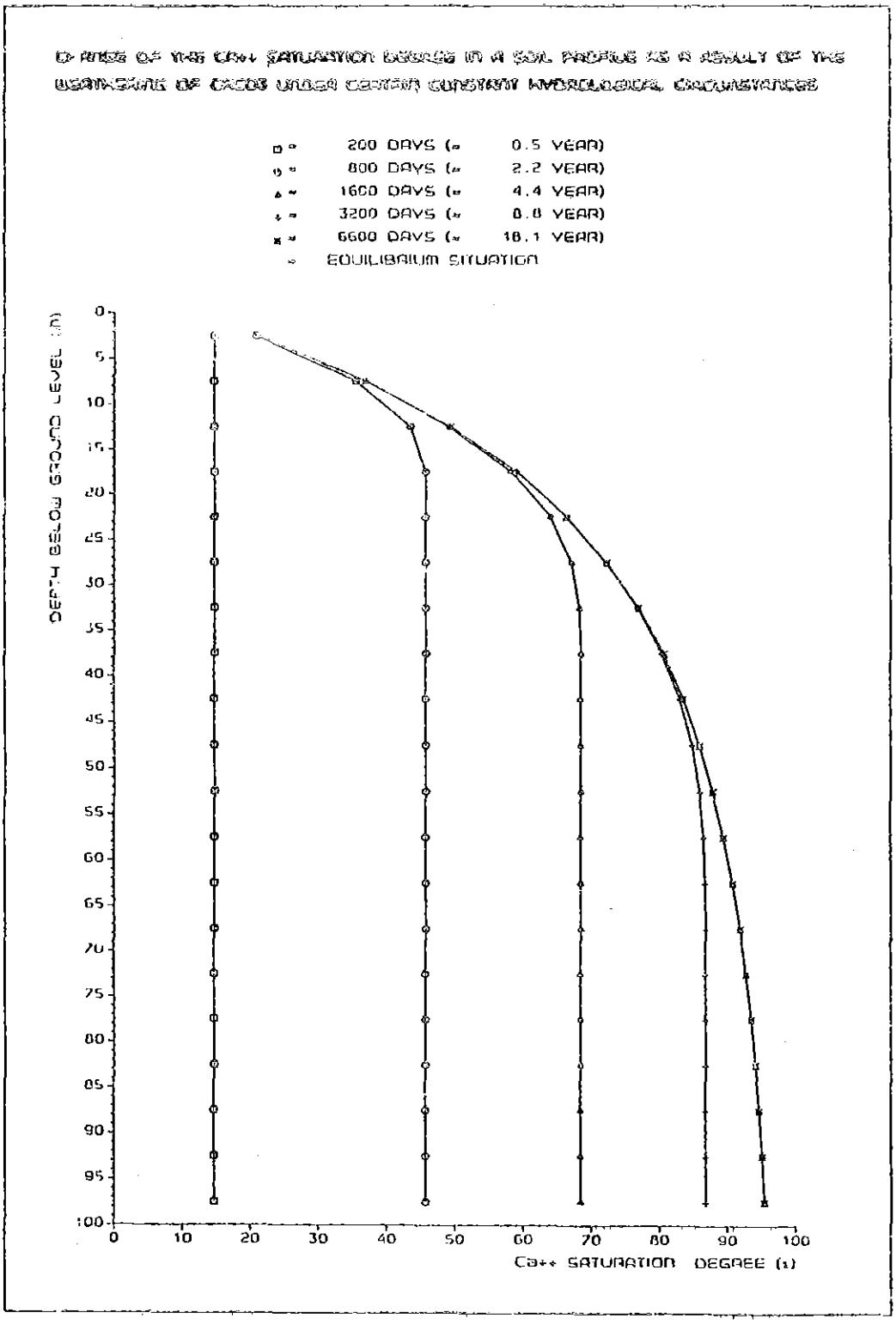

Fig. 7. Influence of Ts on the realization of the Ca^{++} saturation degree-depth profile Ts = 1,000 s. The values of the other parameters are equal to the values used in the Fig. 5 and 6

An increase in the amount of solid $CaCO_3$ in the soil causes the Ca^{2+} saturation degree depth profiles to steepen. However, when comparing Fig. 5 and 6 it becomes clear that a doubling of the quantity of solid $CaCO_3$ in soil does not result in a doubling of the free Ca^{++} concentration in the bulk solution.

A decrease in flux (percolation velocity) causes an increase in the Ca^{++} concentration in the whole soil column (see Fig. 8, 9 and 10). Consequently the concentration depth profiles will steepen. In fact, the influence of the flux on the development of the concentration depth profiles is opposite to the influence of A. However, a halvation of the flux does not result in a doubling of the Ca^{++} concentration in the bulk solution.

Fig. 11 until 13 show the influence of Ca^{++} feed in the case Ca^{2+} feed is smaller, equals or is bigger than the Ca^{++} initial. Fig. 11 is an example of dilution of the soil solution and Fig. 13 of enrichment. The steady-state equilibrium profiles are steep as a result of the great percolation velocity (1.46 m/year).

Fig. 14, 15 and 16 are examples of dilution of the soil solution. It is striking that in all cases the dilution results in similar equilibrium concentration depth profiles. The initial Ca^{++} concentration in the soil apparently has no influence on the establishment of the steady-state equilibrium concentration depth profiles.

The Fig. 17 until 19 are graphical representations of concentration depth profiles under constant hydrological circumstances for different pH-values. This means that the figures can not be compared direcrly to each other because of different Ce-values. For example, a 80% Ca^{++} saturation degree in Fig. 17 refers to an other absolute Ca^{++} concentration than is the case in Fig. 18 or 19.

Recalculation of the steady-state equilibrium profiles, however, shows that a lower pH-value consequently gives rise to absolute higher Ca^{++} concentrations in the soil profile. This is to be expected, since it is generally acknowledged that under acid circumstances $CaCO_3$ will be weathered more intensily than under basic circumstances.

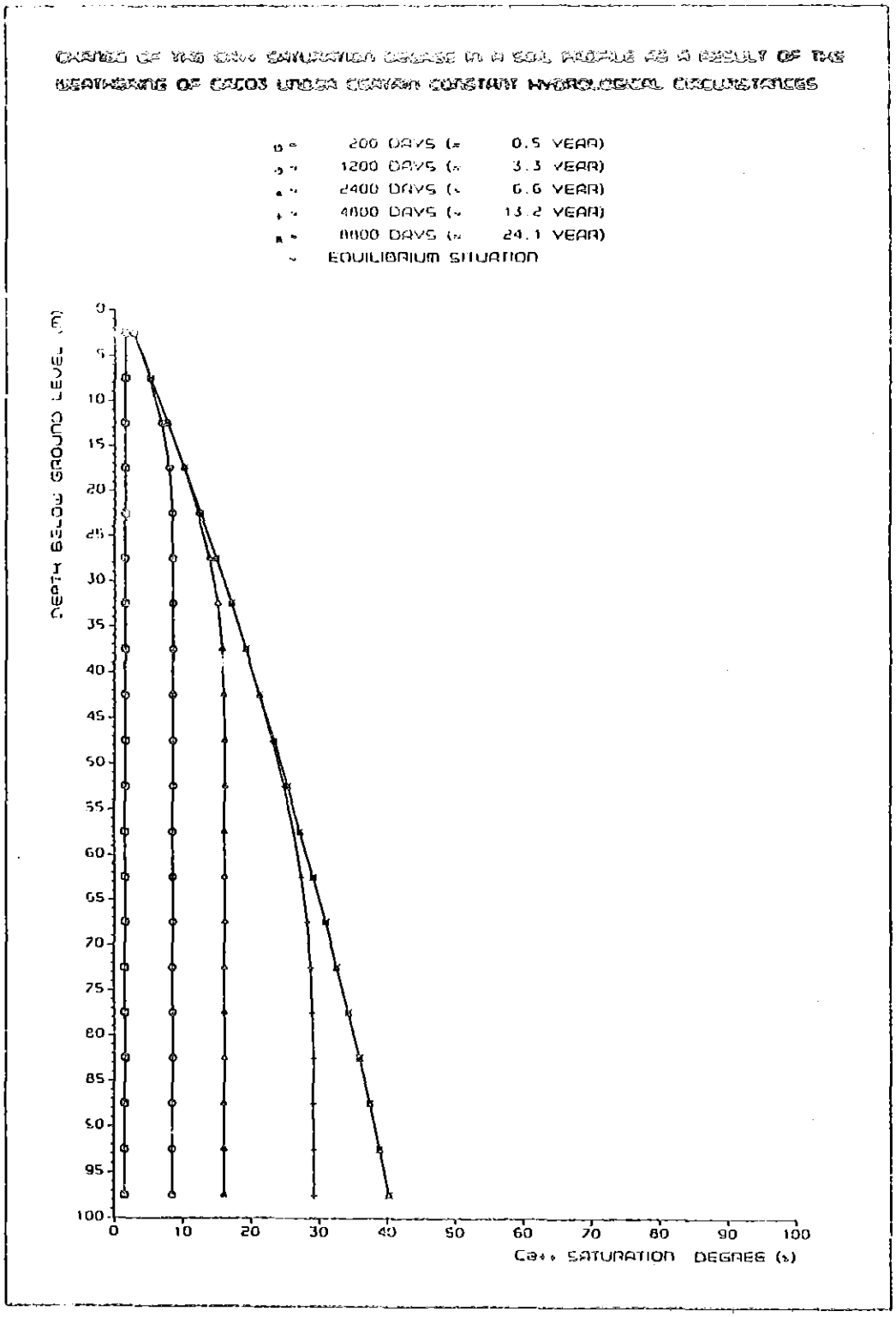

Fig. 8. Influence of the flux on the realization of the Ca^{++} saturation degree depth-profile.q = 0.004 m/day. The values of the other parameters are equal to the values used in the Fig. 9 and 10

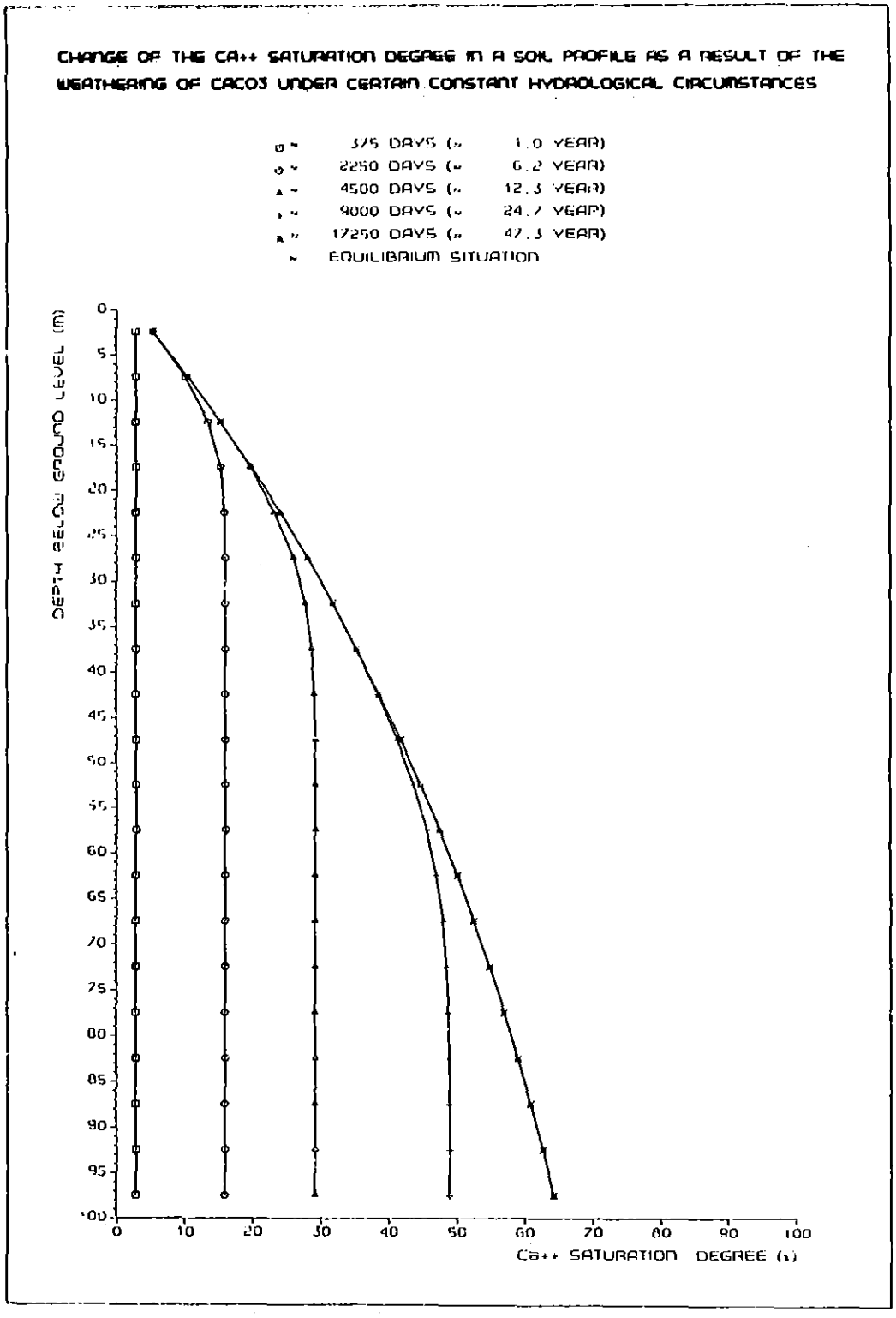

Fig. 9. Influence of the flux on the realization of the Ca^{++} saturation degree-depth profile. q = 0.002 m/day. The values of the other parameters are equal to the values used in the Fig. 8 and 10

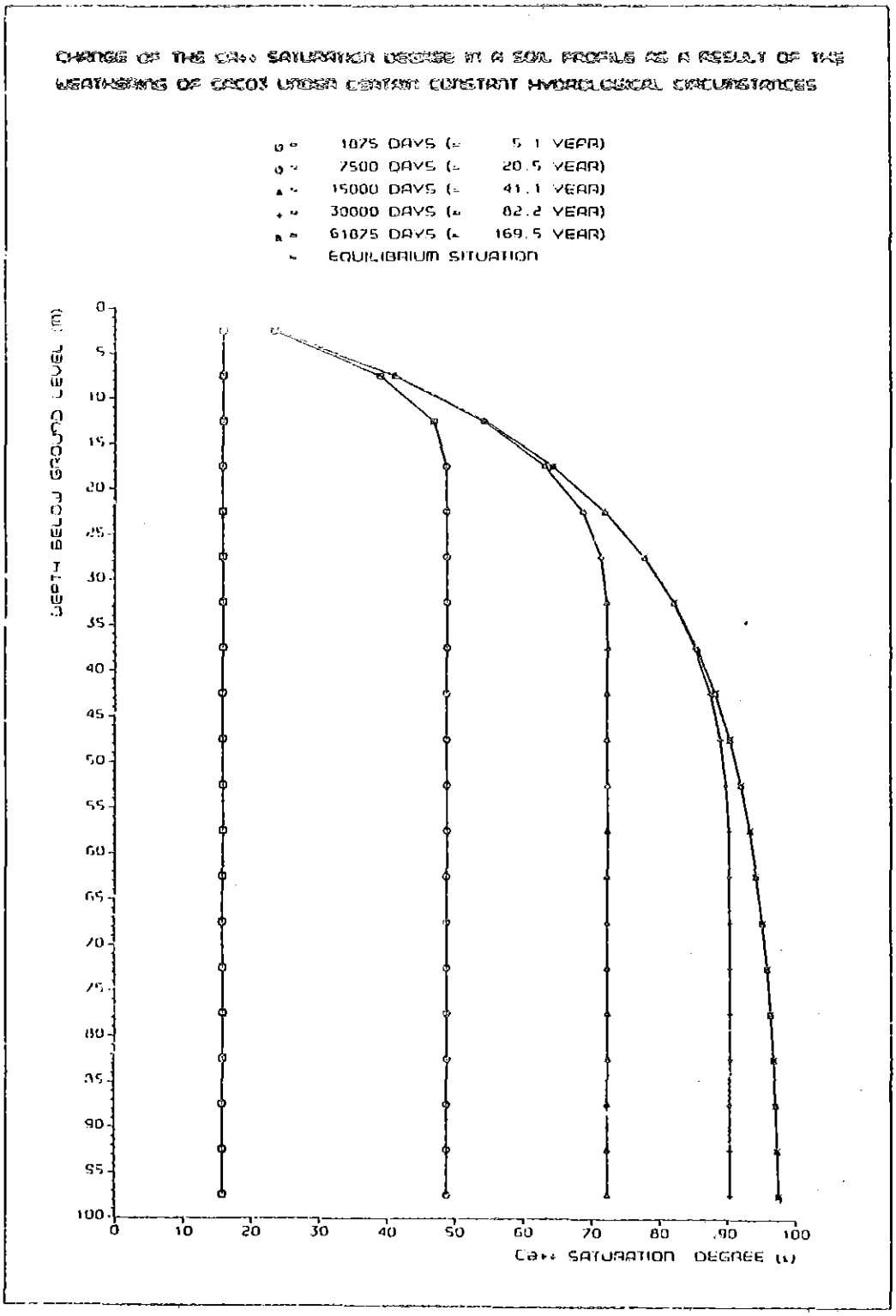

Fig. 10. Influence of the flux on the realization of the Ca^{++} saturation degree-depth profile. q = 0.0004 m/day. The values of the other parameters are equal to the values used in the Fig. 8 and 9

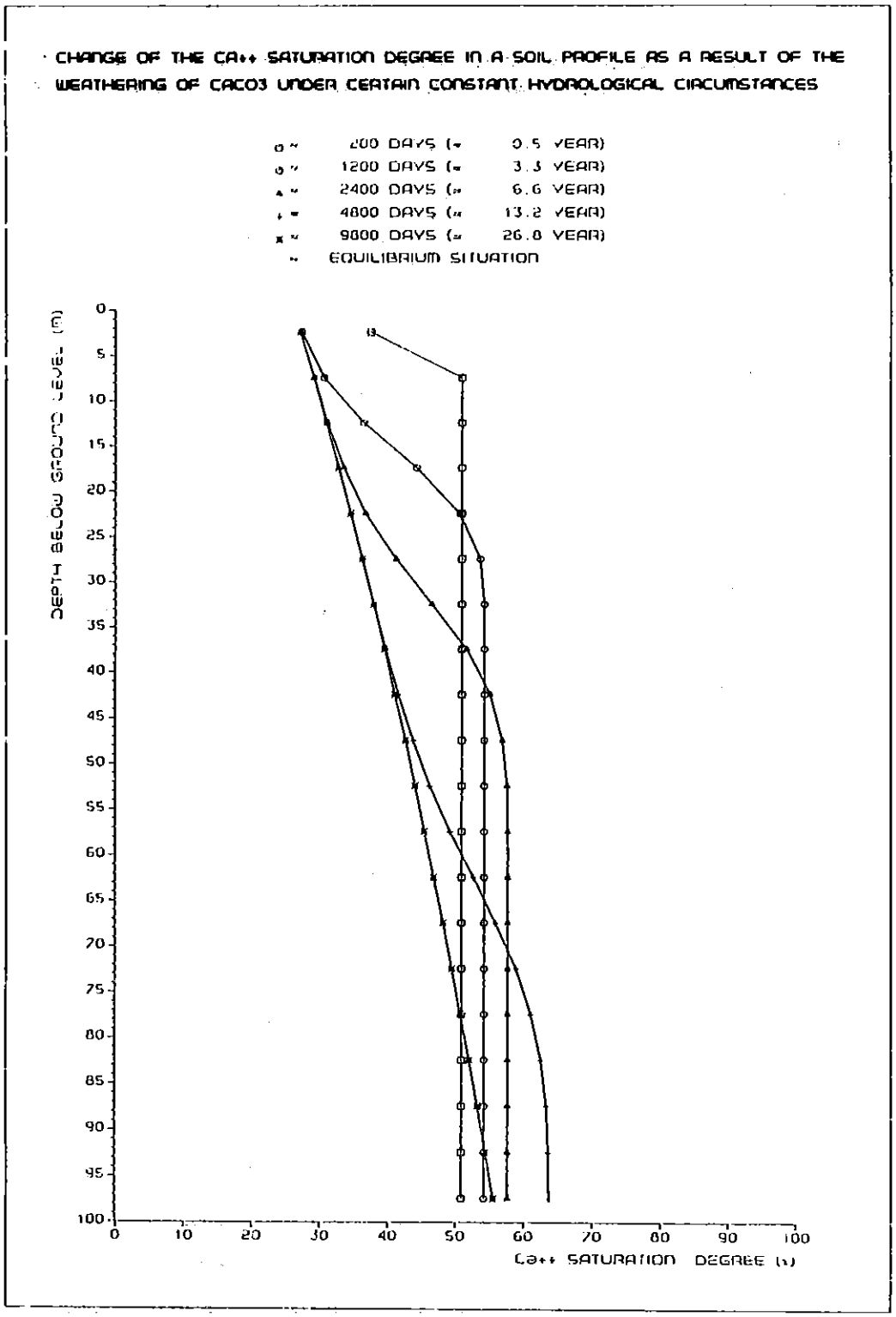

Fig. 11. Influence of Ca^{++} feed on the realization of the Ca^{++} saturation degree-depth profile. Ca^{++} feed = 0.024 mole/l. The values of the other parameters are equal to the values used in the Fig. 12 and 13

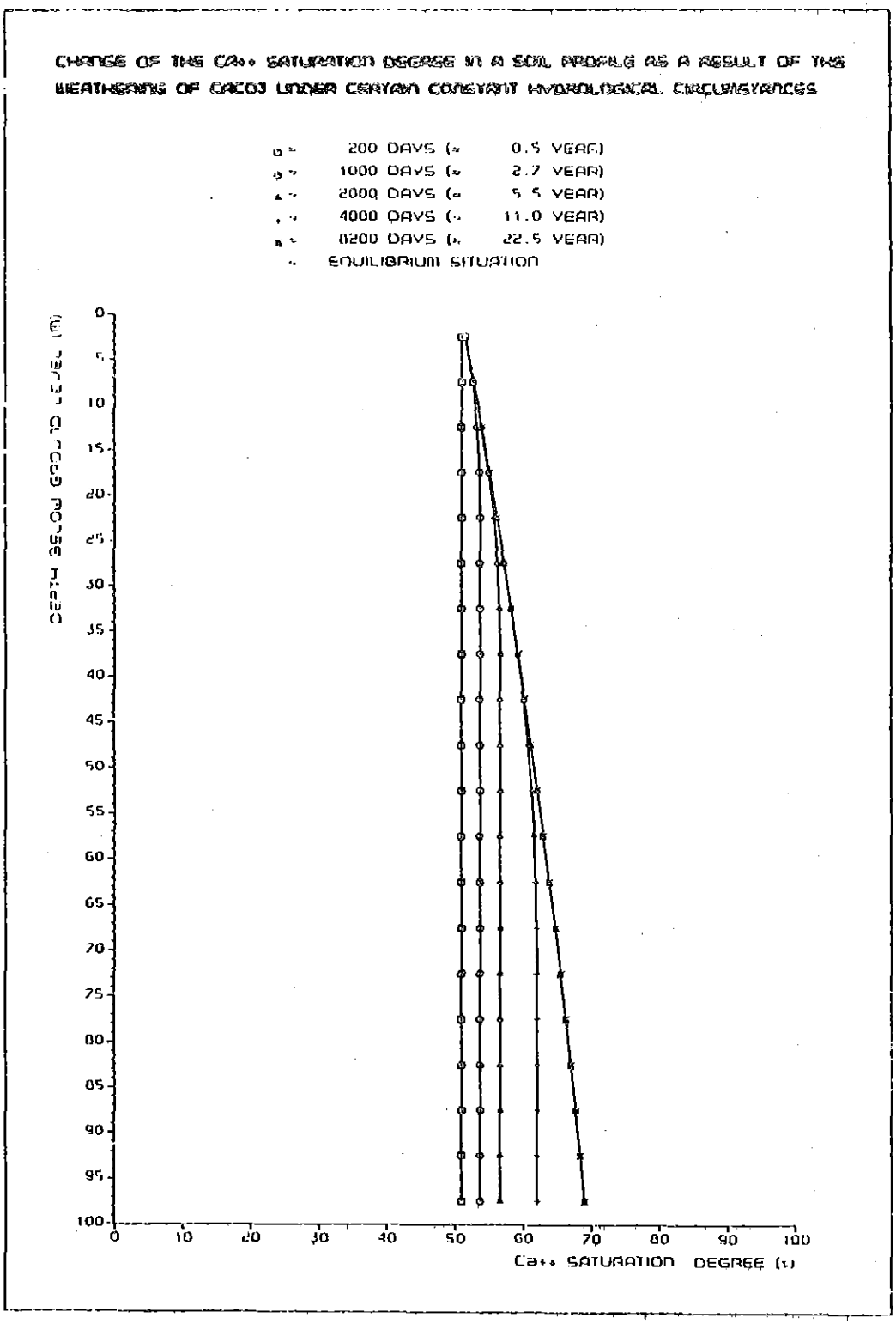

Fig. 12. Influence of Ca^{++} feed on the realization of the Ca^{++} saturation degree-depth profile, Ca^{++} feed = 0.048 mole/l. The values of the other parameters are equal to the values in the Fig. 11 and 13

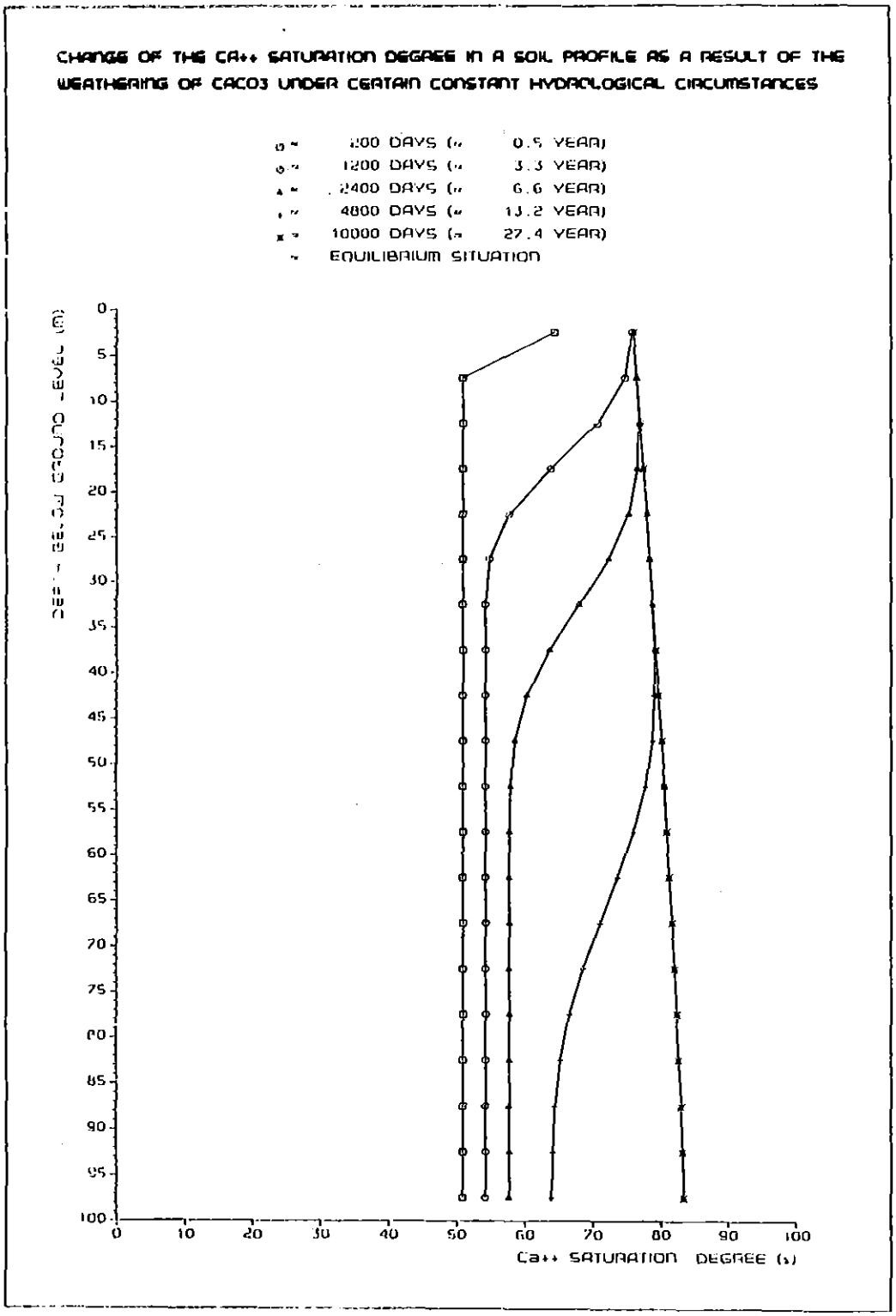

Fig. 13. Influence of Ca^{++} feed on the realization of the Ca^{++} saturation degree depth-profile. Ca^{++} feed = 0.072 mole/l. The values of the other parameters are equal to the values used on the Fig. 11 and 12

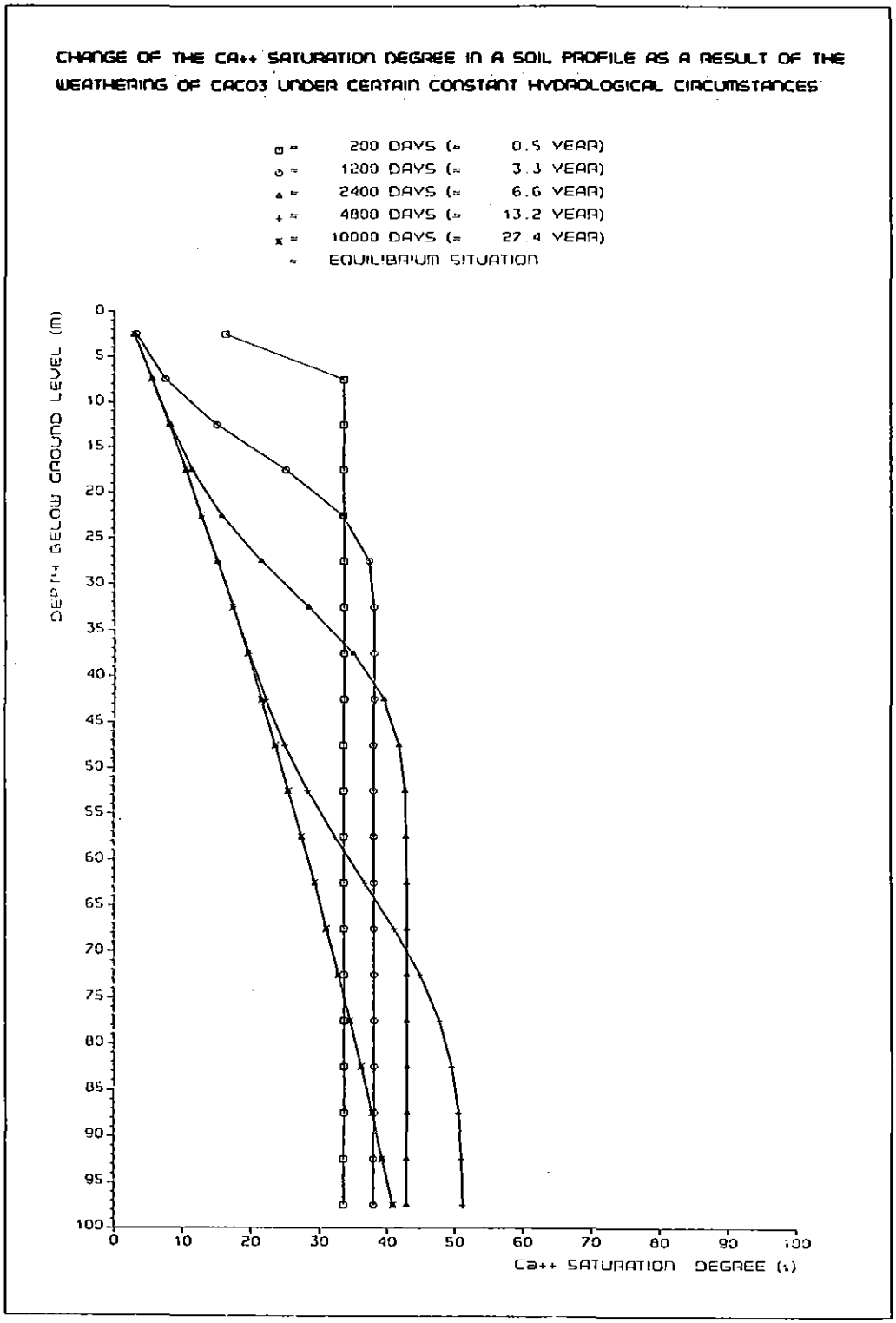

Fig. 14. Influence of Ca^{++} initial on the realization of the Ca^{++} saturation degree-depth profile. Ca^{++} initial = 0.024 mole/l. The values of the other parameters are equal to the values used in the Fig. 15 and 16

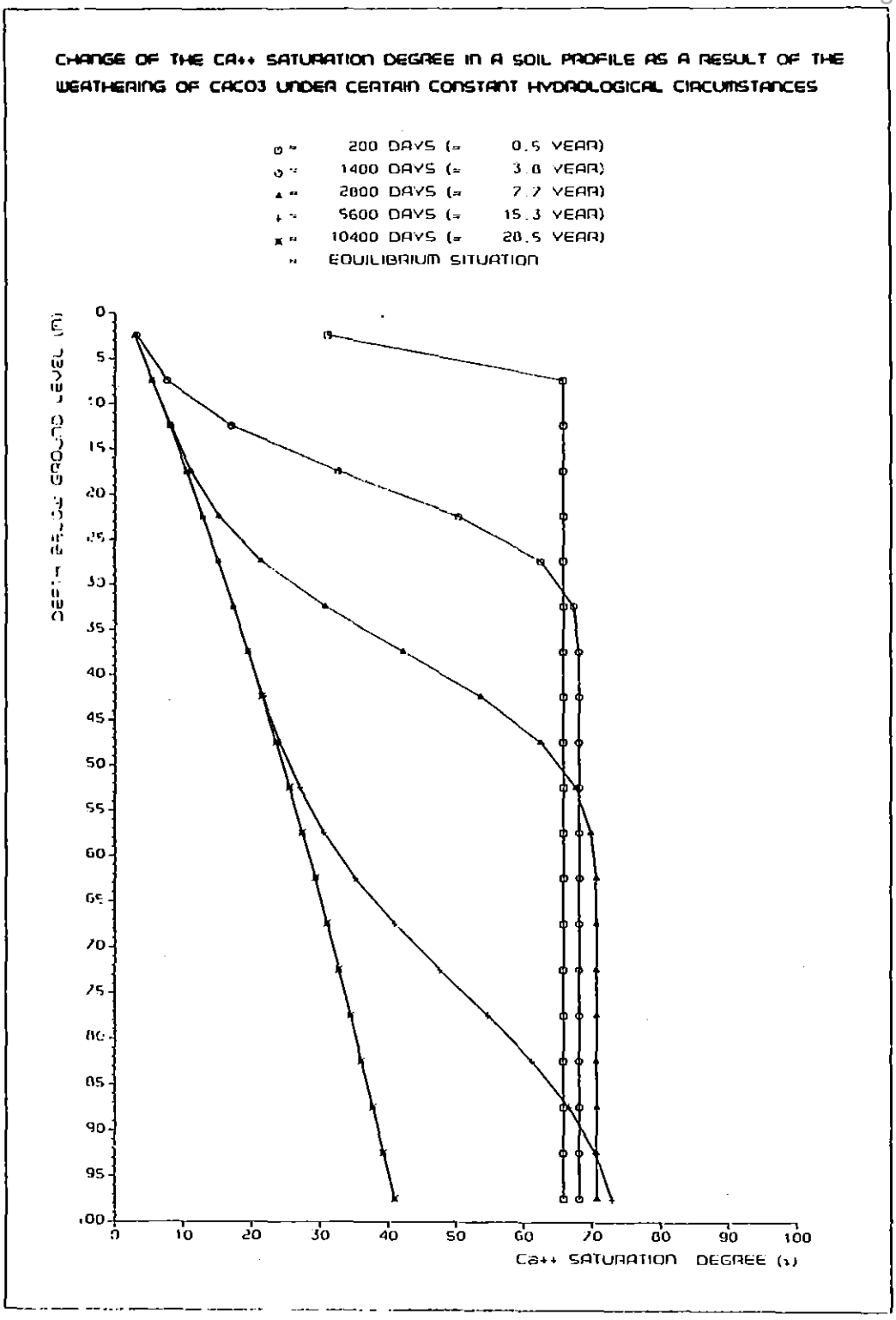

Fig. 15. Influence of Ca^{++} initial on the realization of the Ca^{++} saturation degree-depth profile, Ca^{++} initial = 0.048 mole/1. The values of the other parameters are equal to the values used in the Fig. 14 and 16

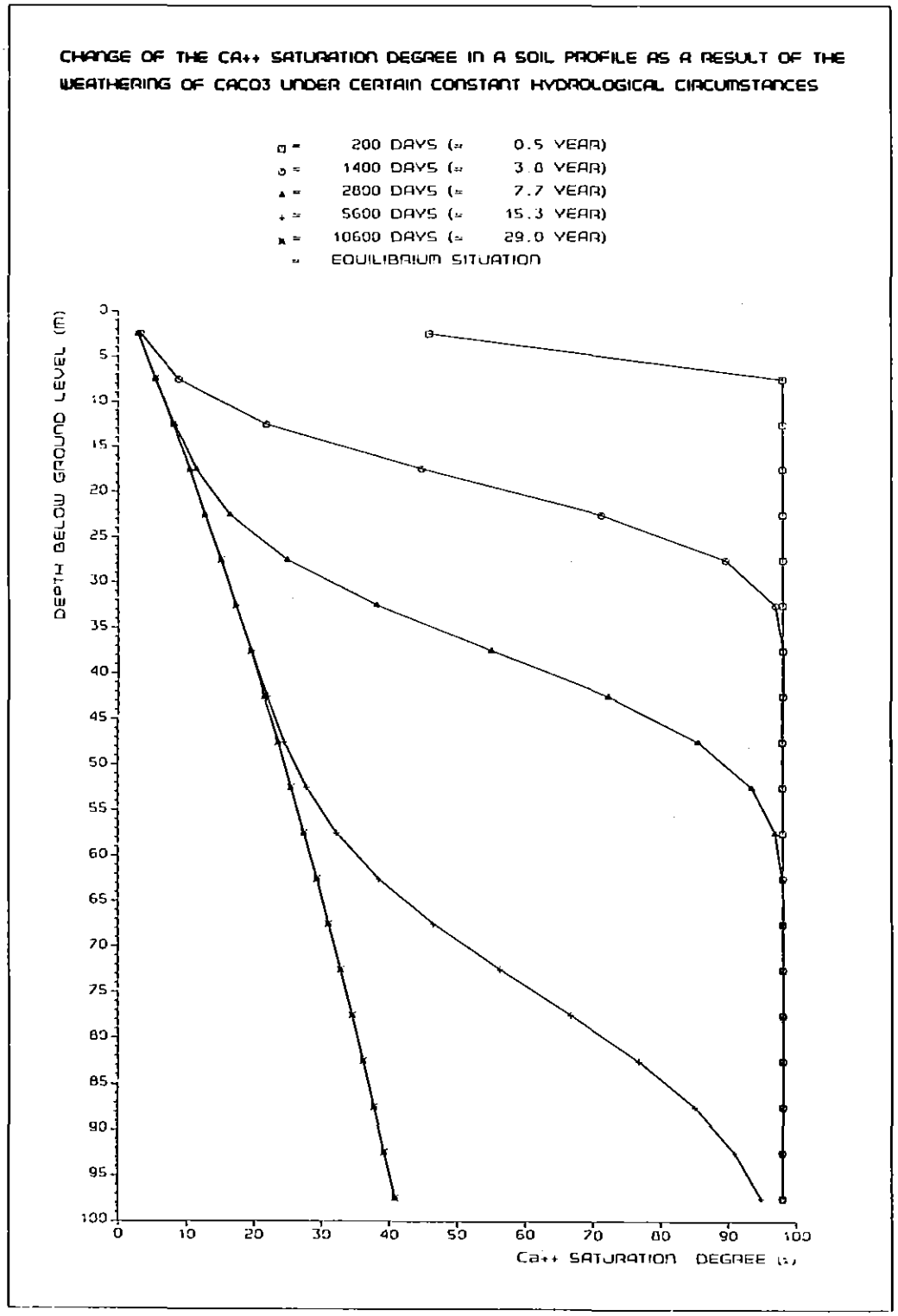

Fig. 16. Influence of Ca^{++} initial on the realization of the Ca^{++} saturation degree-depth profile. Ca^{++} initial = 0.072 mole/l. The values of the other parameters are equal to the values used in the Fig. 14 and 15

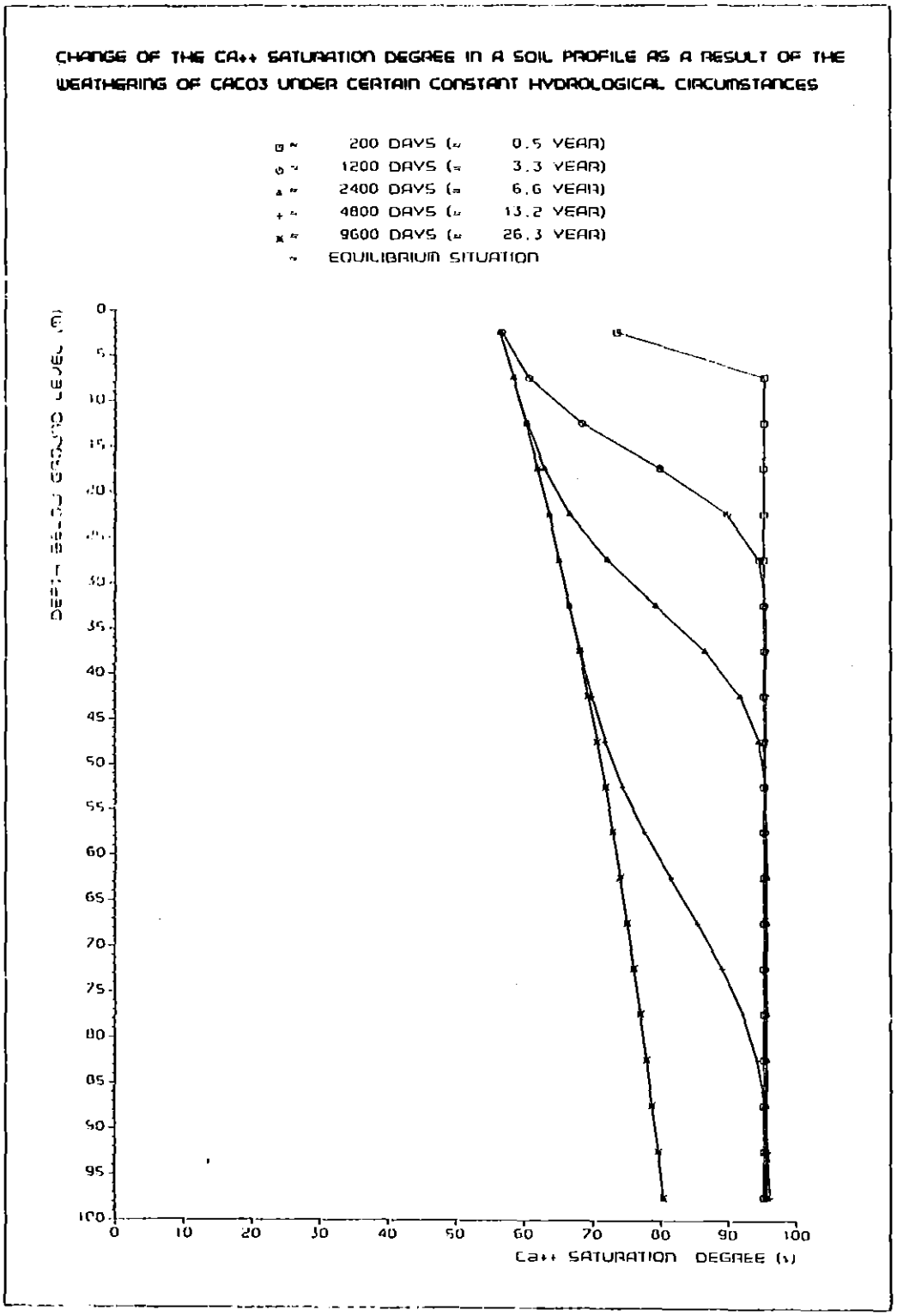

Fig. 17. Influence of the pH on the realization of the Ca^{++} saturation degree-depth profile.pH = 6.0. The values of the other parameters are equal to the values used in the Fig. 18 and 19

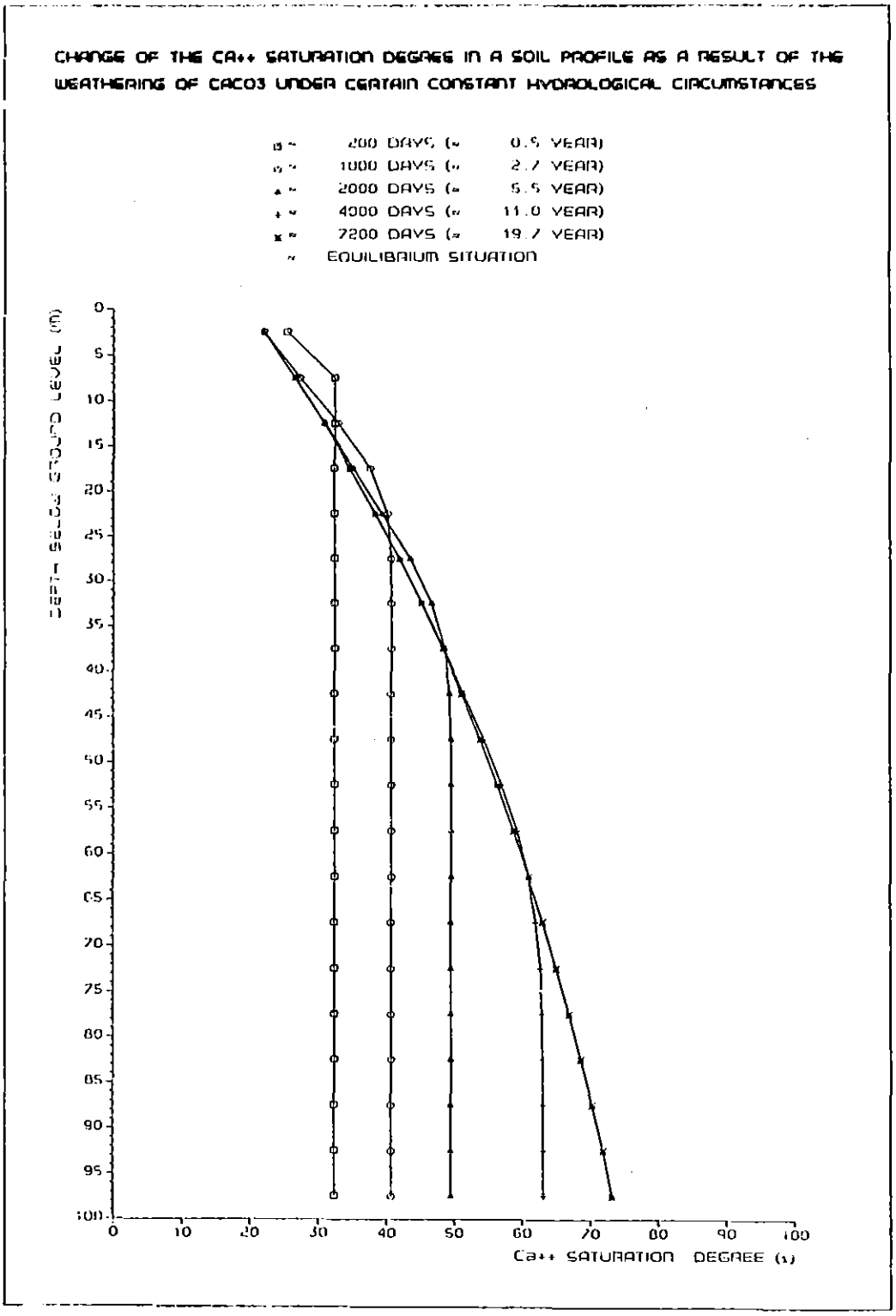

Fig. 18. Influence of the pH on the realization of the Ca^{++} saturation degree-depth profile. pH = 5.5. The values of the other parameters are equal to the values used in the Fig. 17 and 19

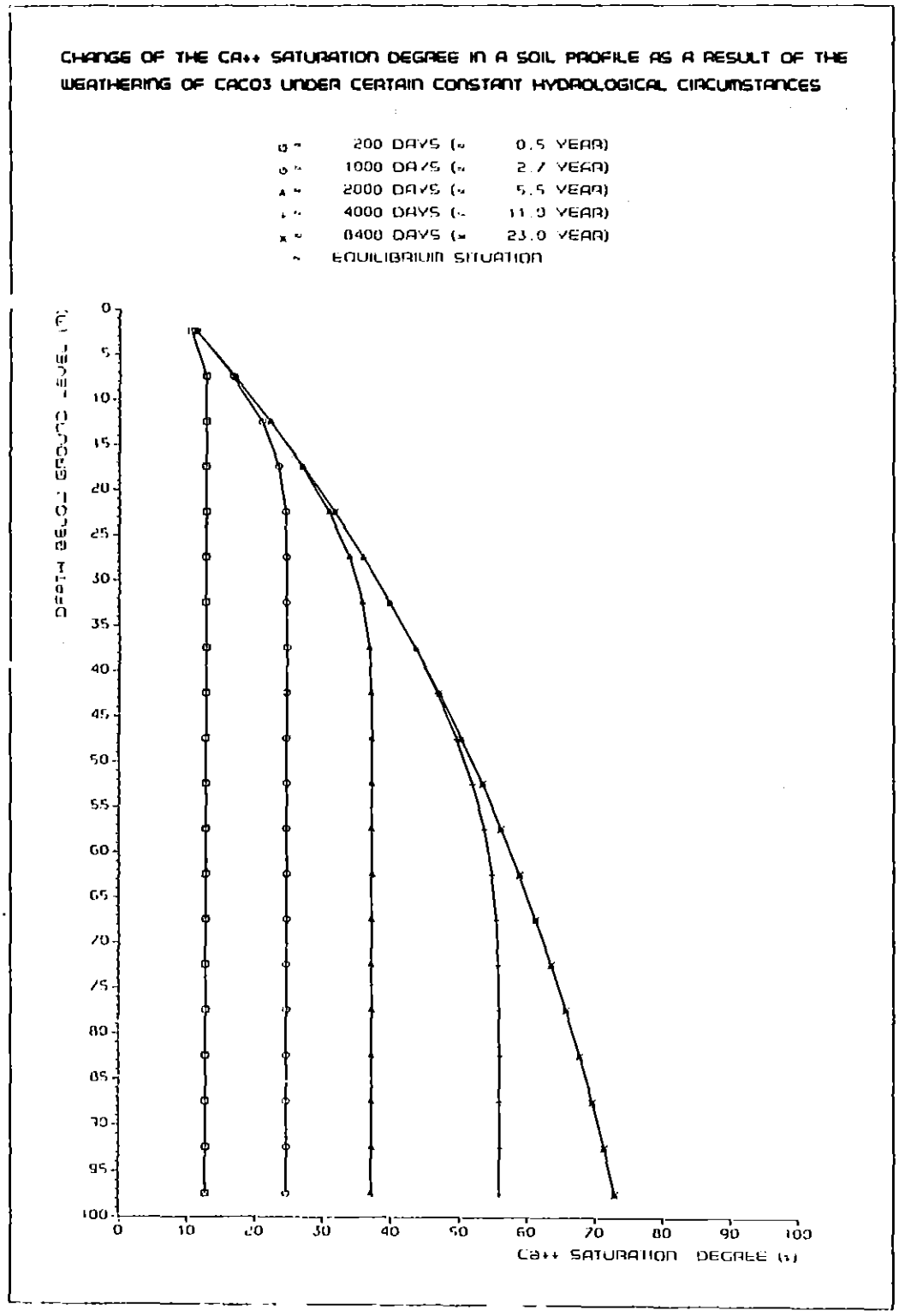

Fig. 19. Influence of the pH on the realization of the Ca^{++} saturation degree-depth profile. pH = 5.0. The values of the other parameters are equal to the values used in the Fig. 17 and 18

6. RESULTS

Calculations are carried out with field data, obtained by the RIVM the Netherlands, and are graphically represented in the Fig. 20 through 27. The figures show both the measured field data and the equilibrium Ca^{++} saturation degree depth profiles as calculated by the $CaCO_3$-weathering model.

All the bore-holes are situated in the High-Veluwe area. Since it is an infiltrating area the flow direction of the percolating water will be mainly vertical.

The pH and HCO_3^--concentration values measured in the separate bore-holes does not change much at different depths. This implies that the bore-holes are pre-eminently suitable for testing the model. The (actual) $CaCO_3$-content is usually not known and is therefore optimized in such way that the calculated concentration depth profiles fit the measured field data in the most proper way.

Besides values of Ts it is necessary to know values for the following variables in order to calculate the equilibrium concentration depth profiles:

flux q	- considered as a constant (0.0008 m/day)
Ca^{2+} feed	- considered as a constant (0.00004 mole/l)
Ca^{2+} initial	- considered as a variable per bore-hole (does not influence the calculated equilibrium concentration depth profile)
pH	- considered as a variable per bore-hole (field data used)
HCO_3^-	- considered as a variable per bore-hole (field data used)

It is possible to consider the hydrological variables flux q and Ca^{++} feed as constants because all the used bore-holes are situated in the central part of the Netherlands.

Table 5 shows all the data per bore-hole used in the calculations.

As can be seen in Table 5 the value of Ts is in general rather high. This consequently means that the amount of solid $CaCO_3$ in the bore-holes is predominantly low. A Ts-value of 20,000 corresponds with 45 cm^2 $CaCO_3/cm^3$ soil, a Ts-value of 1,000,000 with 0.091 cm^2 $CaCO_3/cm^3$ soil. Considering a soil consisting of grains with constant radius of 50 µm and uniform specific gravity it follows that Ts 10,000 and Ts 1,000,000 roughly correspond with respectively 1.1 and 0.022 weight

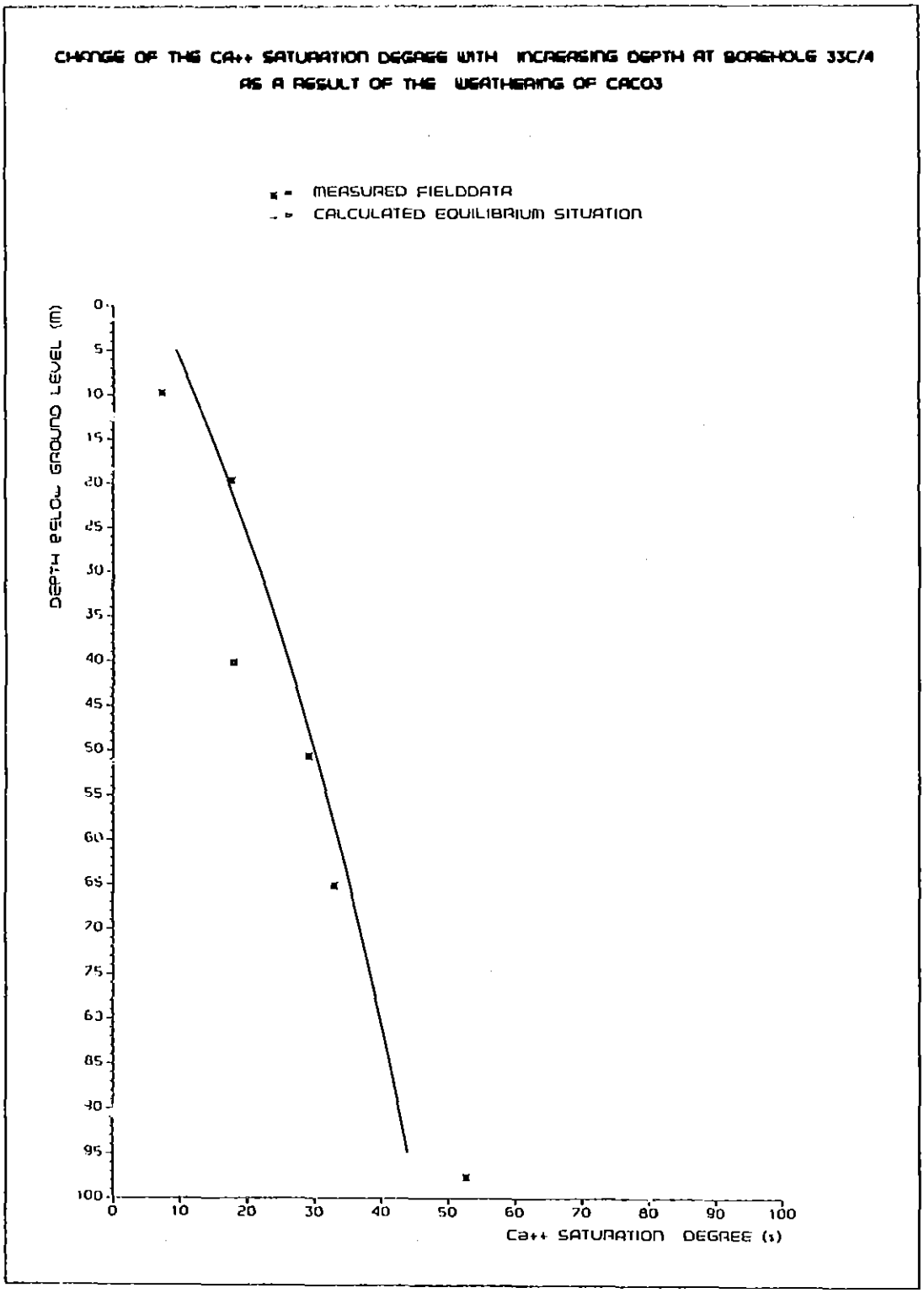

Fig. 20. Ca^{++} saturation degree versus depth at borehole 33C/4

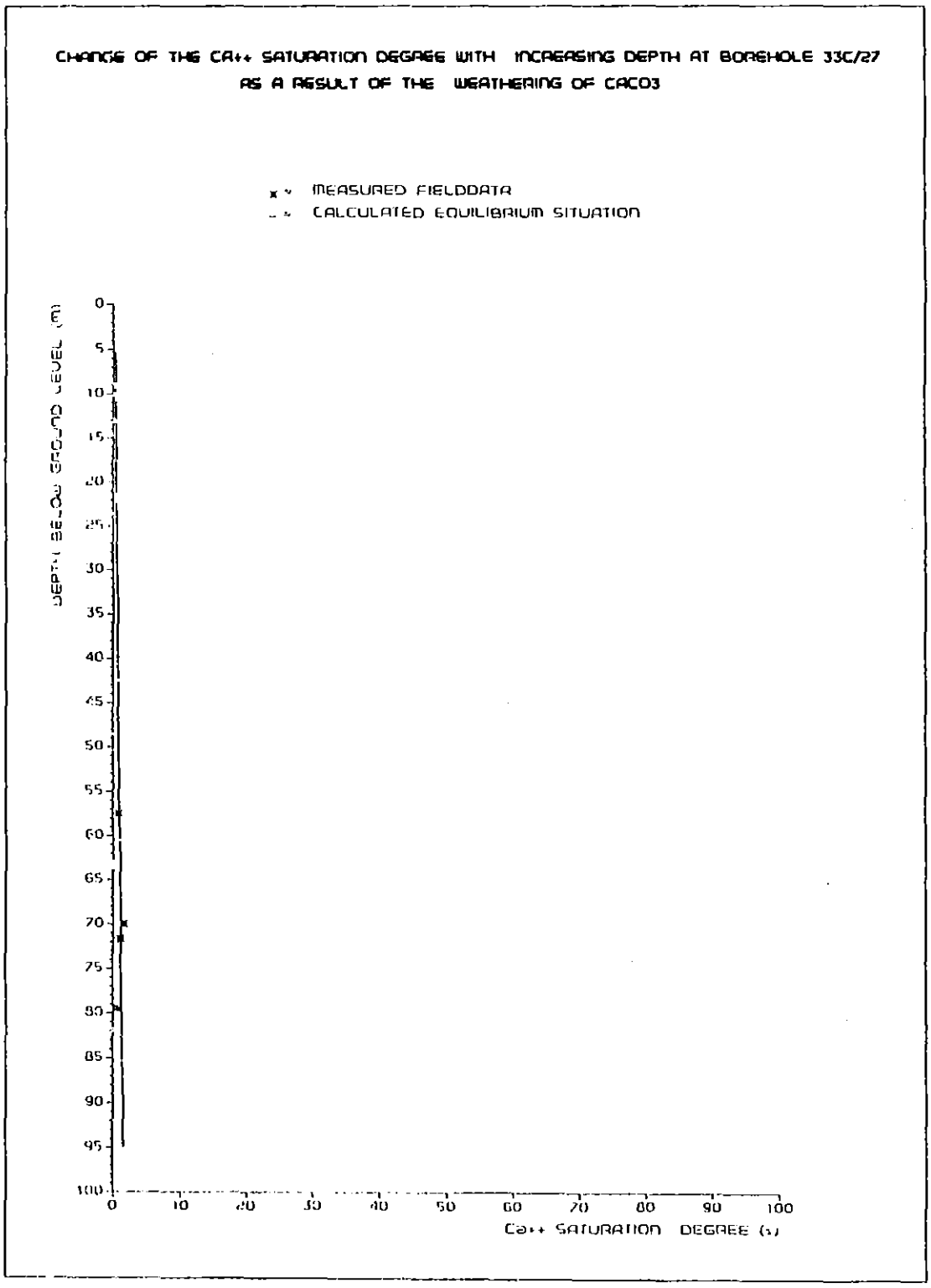

Fig. 21. Ca^{++} saturation degree versus depth at borehole 33C/27

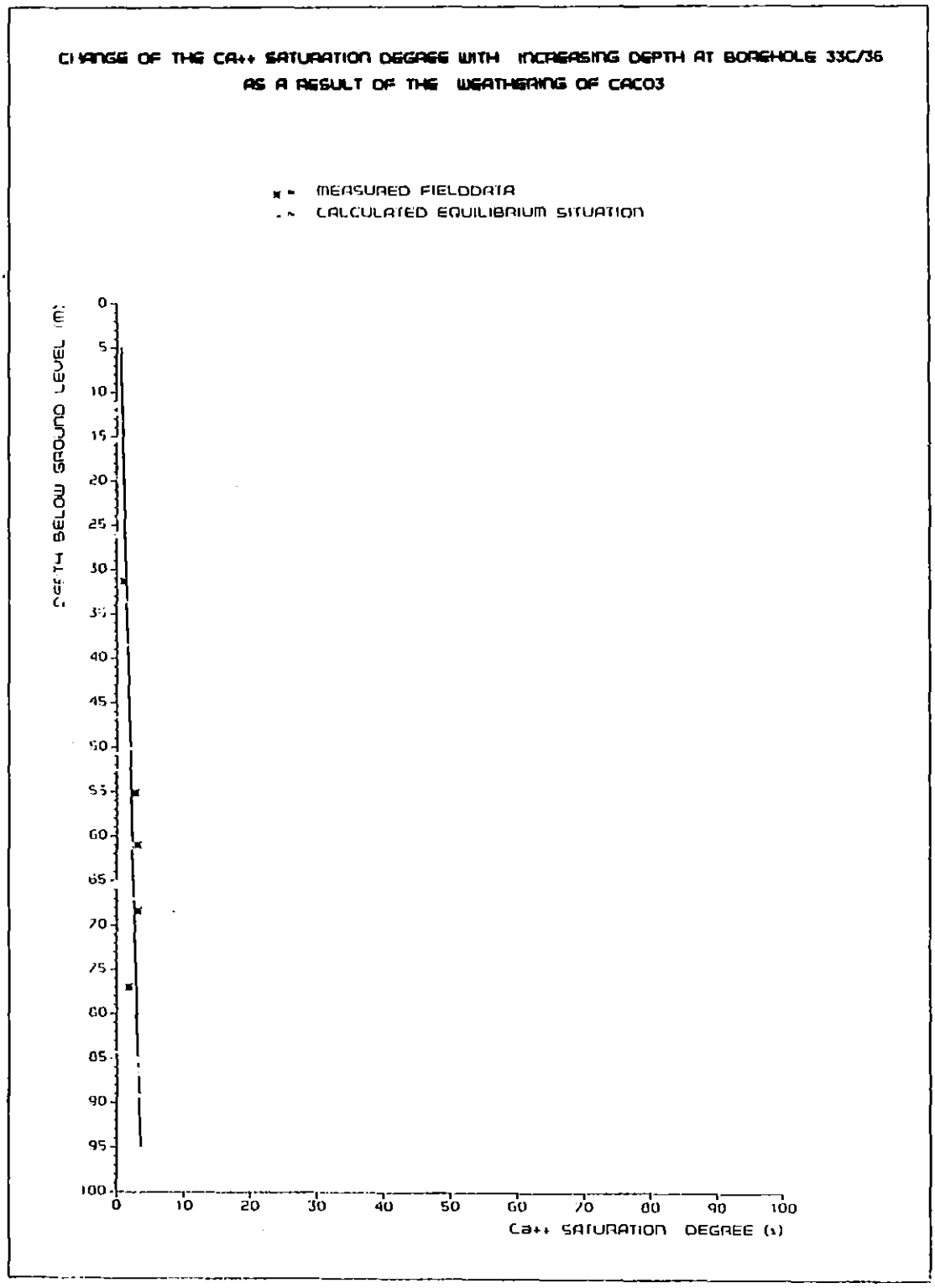

Fig. 22. Ca^{++} saturation degree versus depth at borehole 33C/36

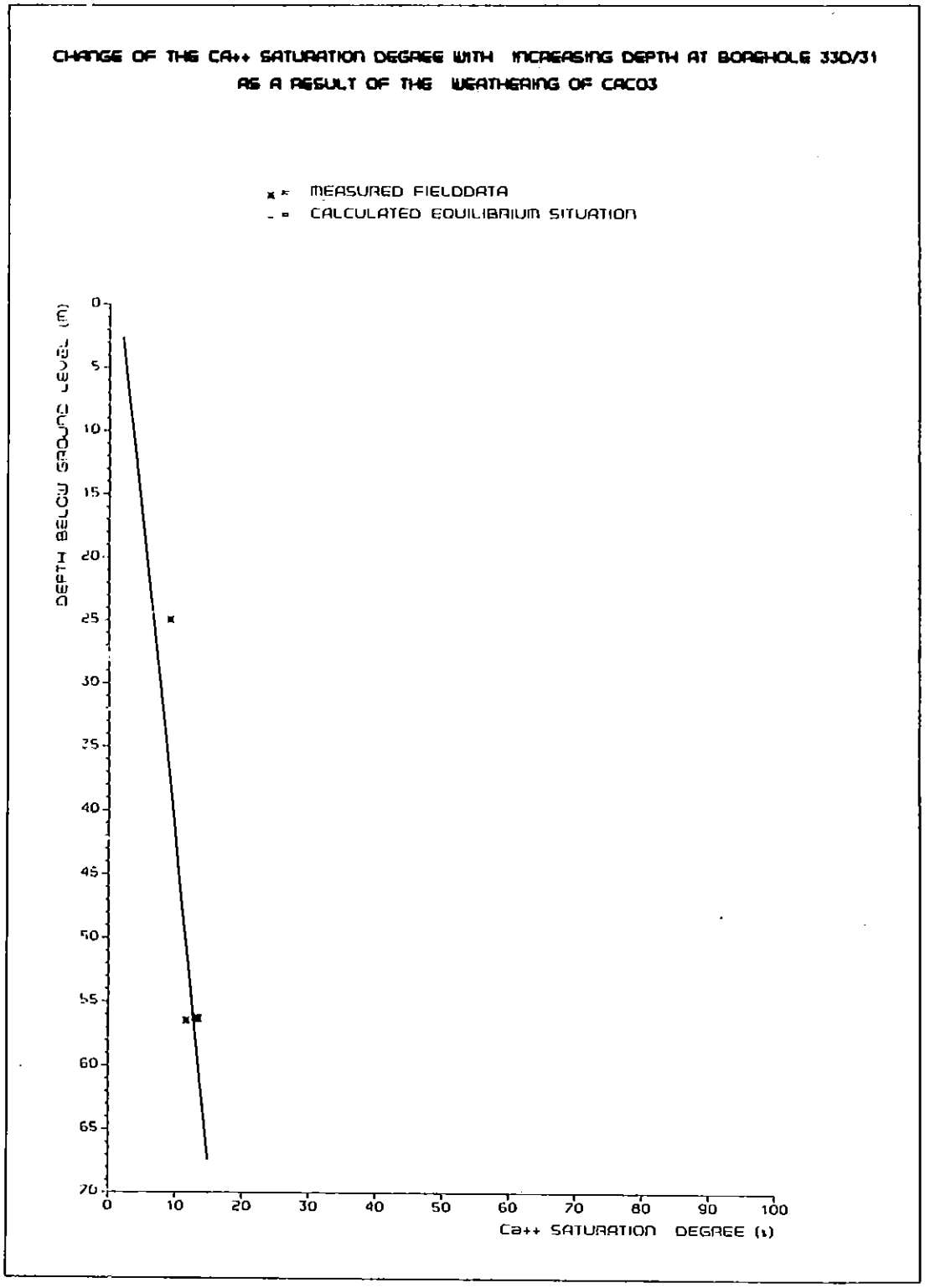

Fig. 23. Ca^{++} saturation degree versus depth at borehole 33D/31

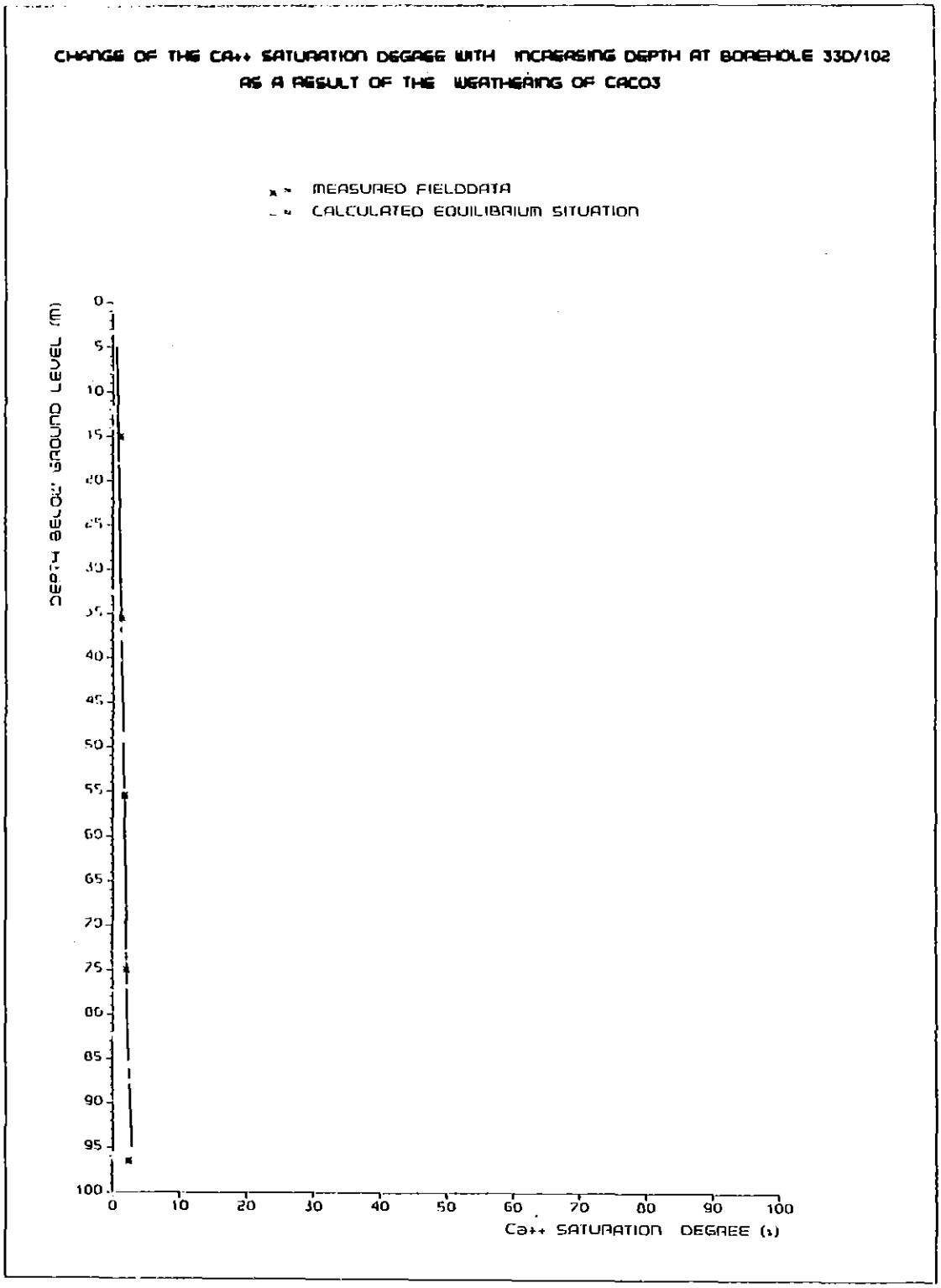

Fig. 24. Ca^{++} saturation degree versus depth at borehole 33D/102

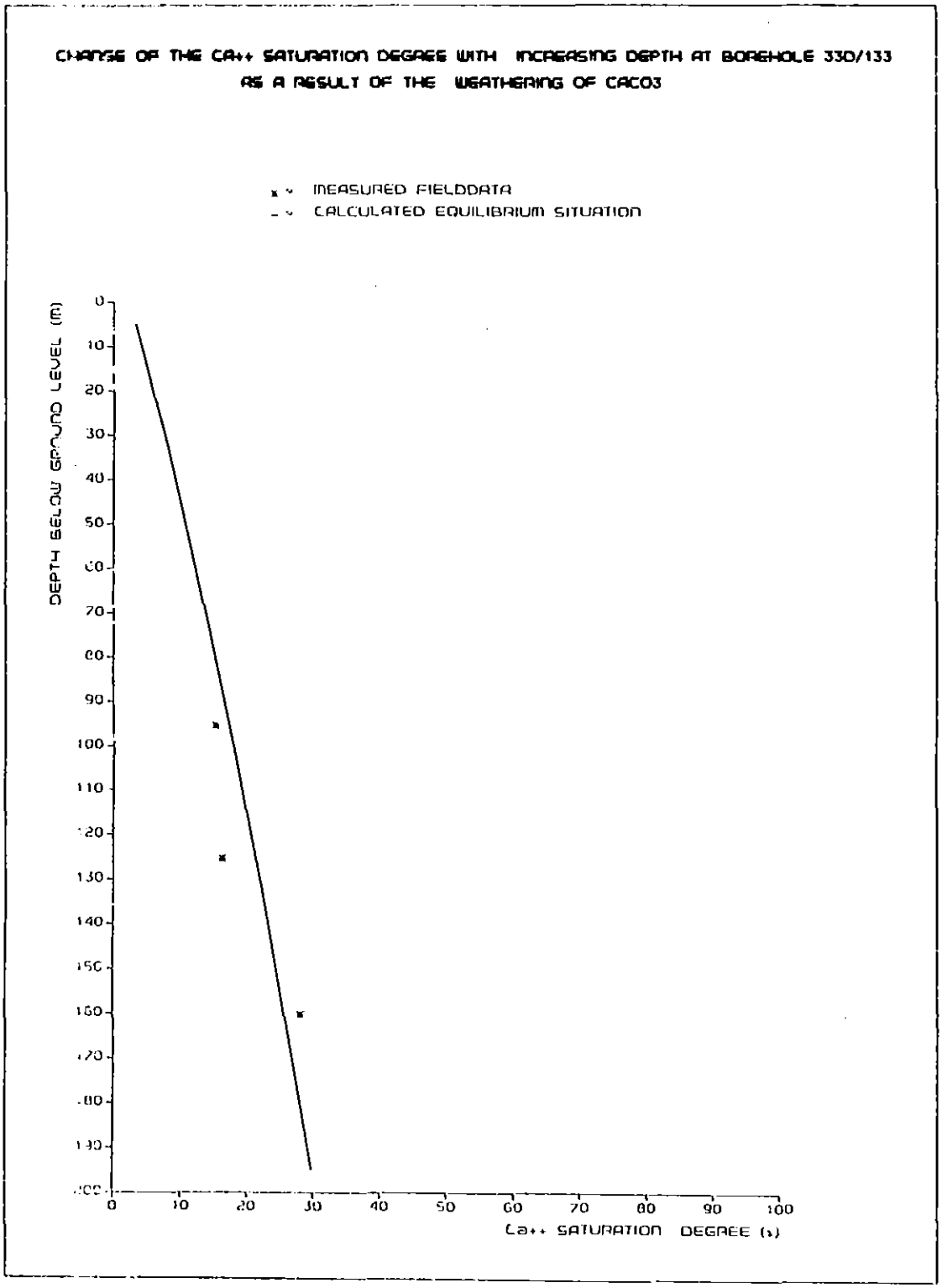

Fig. 25. Ca^{++} saturation degree versus depth at borehole 33D/133

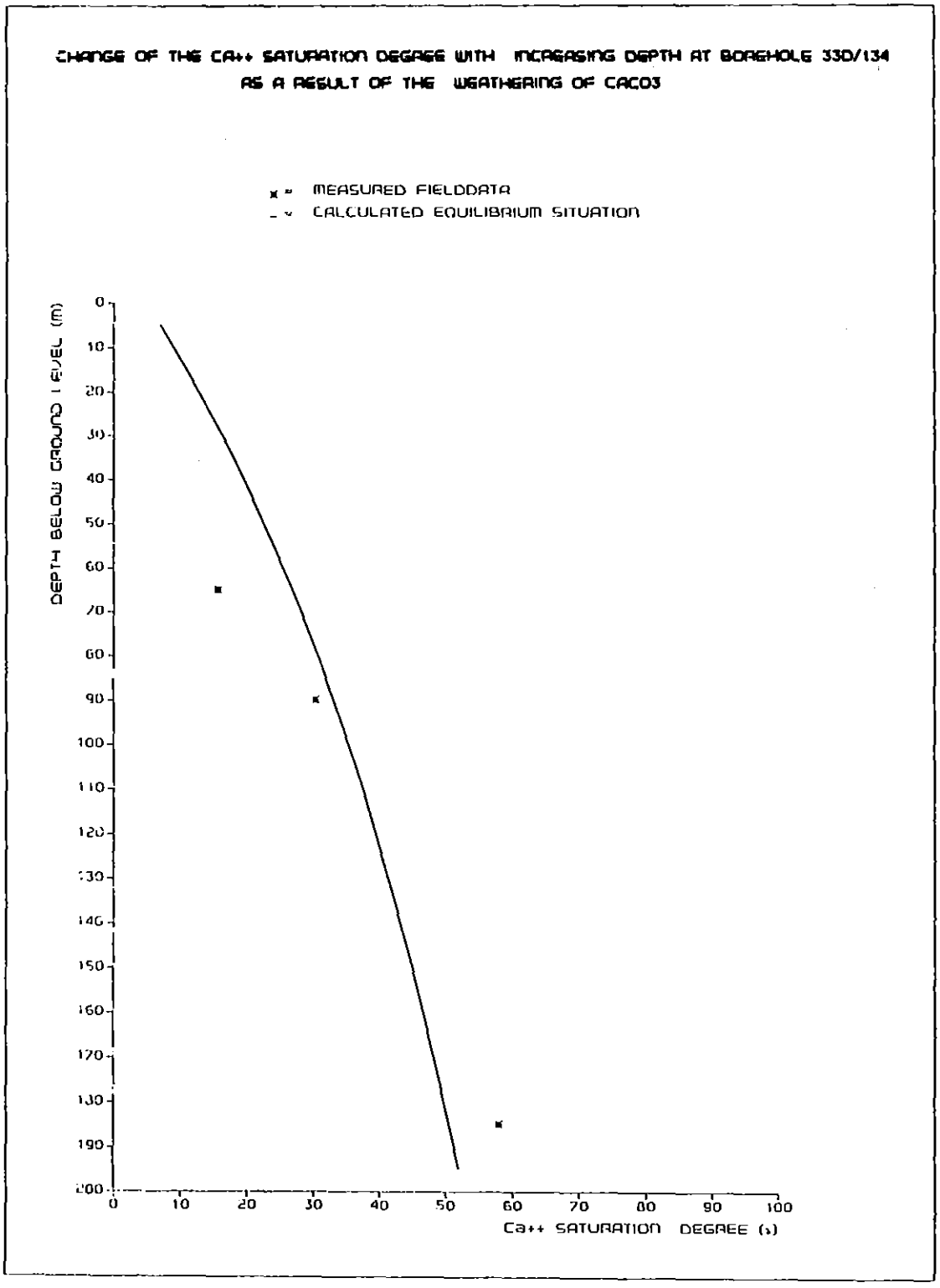

Fig. 27. Ca^{++} saturation degree versus depth at borehole 33D/134

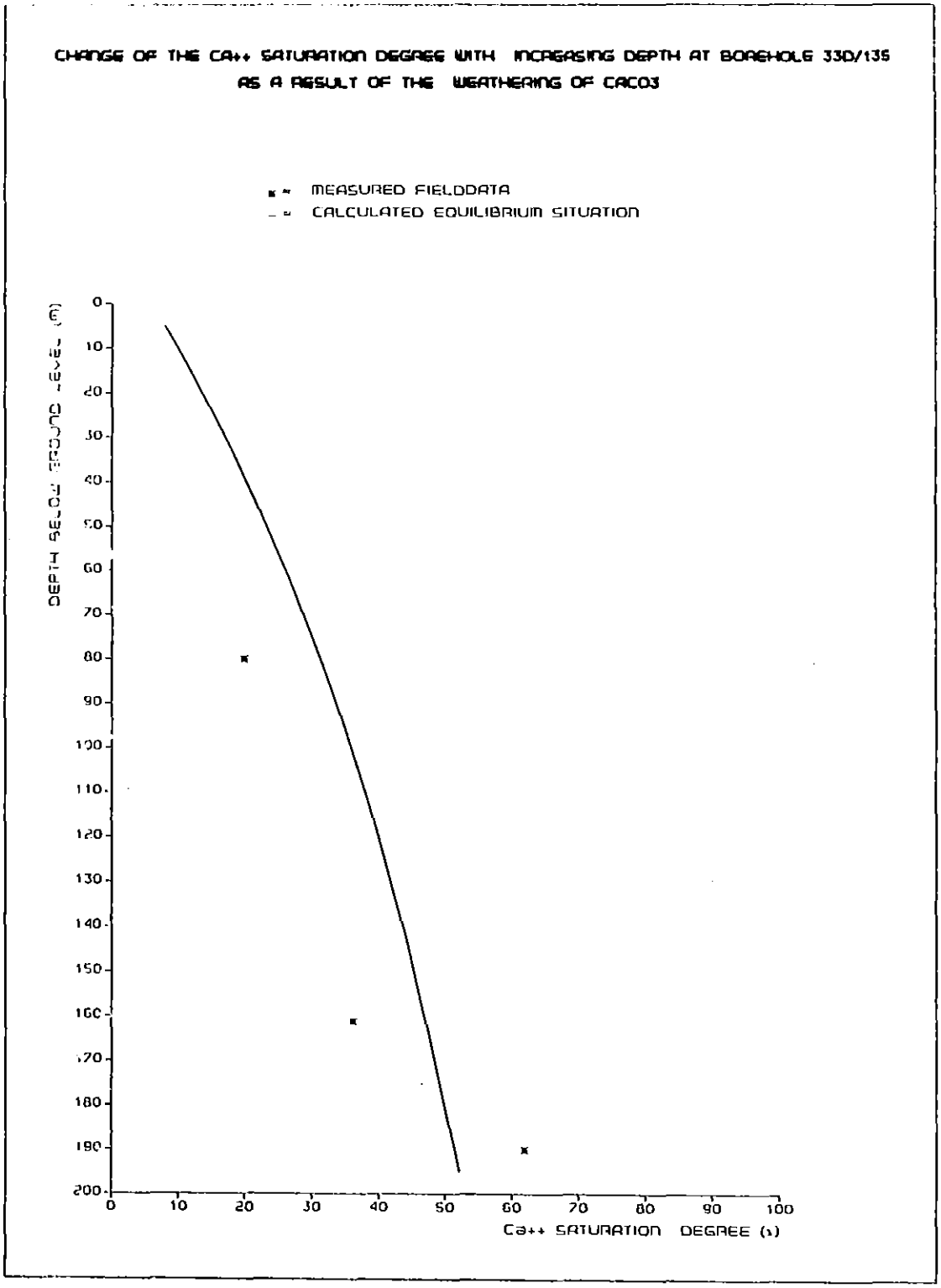

Fig. 27. Ca^{++} saturation degree versus depth at borehole 33D/135

Table 5. Data used to calculate the Ca^{++} saturation degree depth profiles at different boreholes situated in the High Veluwe Area

Borehole No.	Altitude (m+NAP)	Screen depth below land surface (m)	Por. (-)	Flux (m/day)	Ca^{++} feed (mole/l)	Ca^{++} initial (mole/l)	pH (-)	HCO_3^- (mole/l)	Ca^{++} satur. = Ce (mole/l)	Ts (s)	A (cm^2/cm^3)	Weight percentage $CaCO_3$ in soil (%)
33C/4	33.27	178.20	0.3	0.0008	0.00004	0.00024	7.80	0.0013	0.0012	12,000	7.576	1.85
33C/27	59.00	80.50	0.3	0.0008	0.00004	0.0110	6.93	0.0003	0.0330	2,000,000	0.046	0.01
33C/36	59.30	79.10	0.3	0.0008	0.00004	0.0045	7.00	0.0007	0.0136	750,000	0.121	0.03
33D/31	16,00	61.00	0.3	0.0008	0.00004	0.0015	7.07	0.0018	0.0045	75,000	1.212	0.30
33D/102	±30	136.00	0.3	0.0008	0.00004	0.0060	6.94	0.0009	0.0129	1,000,000	0.091	0.02
33D/133	50.70	172.00	0.3	0.0008	0.00004	0.0006	7.37	0.0016	0.0025	70,000	1.299	0.32
33D/134	56.71	201.00	0.3	0.0008	0.00004	0.0003	7.58	0.0019	0.0014	20,000	4.545	1.11
33D/135	63.30	196.00	0.3	0.0008	0.00004	0.0004	7.60	0.0022	0.0011	17,000	5.348	1.31

percentage of $CaCO_3$ per unit of soil. The $CaCO_3$ (weight-)percentages given by the Soil Survey Institute of the Netherlands (1965) for the top soil layers of the High Veluwe area vary from 0.5 until 0.0%.

The calculated values which are shown in the various figures represent steady-state equilibrium situations. Changes of pH or HCO_3^- concentrations, for example as a result of acidification of the rain, will cause a corresponding change in the Ca^{++} saturation depth profiles in the soil.

However, the $CaCO_3$ weathering model as defined in Chapter 4 calculates with constant soil pH and HCO_3^- concentrations and is therefore only useful for areas where such conditions prevail.

The deviations from the measured field data with regard to the calculated equilibrium lines are mainly caused by slight variations in the soil pH and HCO_3^- concentrations, which directly result in changes in the Ca^{++} saturation concentration. Nevertheless, it can be seen that their exist a good similarity between the calculated equilibrium profiles and the measured field data.

CONCLUSIONS

The dissolution (weathering) of soil minerals can have an appreciable effect on soil water chemistry.

The contribution from soil minerals to the soil solution consists primarily of calcium, magnesium and bicarbonate (AMRHEIN, 1984). As a result, infiltrating water in soils will undergo a certain grade of Ca^{++} enrichment per unit of time. The grade of enrichment depends on the amount of solid $CaCO_3$ in the soil, the velocity of the percolating water, the value of the pH, the HCO_3^- concentration, the temperature etc.

The formulated $CaCO_3$ weathering model is based on the realization of a dynamic equilibrium situation. The calculated steady-state situation is the result of the interaction between the chemical rate constant Kc (i.e. the degree in which a mineral can be dissolved/weathered), the hydrological circumstances (i.e. the degree in which a component can be transported) and the specific soil conditions (Ts, pH, HCO_3^-, temperature etc.). Realization of the calculated equilibrium situation is consequently a time dependant process.

In the field both under and supersaturated soil water are commonly found (BACK, 1963; SHUSTER and WHITE, 1972; JACKSON and PATTERSON, 1982; SUAREZ, 1977, 1982; PLUMMER and BACK, 1980). The Ca^{++} saturation degrees found in the groundwaters of the High Veluwe area are all under saturated (see Fig. 20 until 27). This is in accordance with the data of HOOGENDOORN (1983) who mentiones undersaturation in the high and increasing saturation in the lower parts of the Veluwe area.

The, for the different bore holes, calculated Ca^{++} saturation depth profiles resemble good with measured field data (see Fig. 20 until 27). In the calculations optimization has taken place with help of the Ts parameter.

The results show that the (actual) weight percentages solid $CaCO_3$ in the soils at the different bore holes vary between 0.01 and 1.8% (see Table 5). This roughly corresponds with the data given by the Soil Survey Institute of the Netherlands (1965).

Intending to calculate Ca^{++} saturation depth profiles in heterogeneous areas it is necessary to adapt the developed model to variable pH and HCO_3^- concentrations.

LITERATURE

AMRHEIN, C., 1984. The effect of an exchanger phase, carbondioxide, and mineralogy on the rate of geochemical weathering. Utah State University, Ph.D., 139 p.

BACK, W., 1963. Preliminary results of a study of calcium carbonate saturation of groundwater in central Florida. In: Int. Ass. Sci. Hydrol., vol. 8, 43-51.

BLÖMER, F., 1985. The mixing-cell transport model - A finite difference approach for solving the convection - dispersion equation. Institute for Land and Water Management Research (ICW), Wageningen, the Netherlands. Nota ICW 1618, 11 p.

BOLT, G.H. and M.G.M. BRUGGENWERT, 1978. Soil chemistry. A. Basic Elements. Elsevier, Amsterdam, 281 p.

GOBRAN, G.R. and S. MIYAMOTO, 1985. Dissolution rate of gypsum in aqueous salt solutions. In: Soil Science, Vol. 140, No. 2, 89-93.

GROENENDIJK, P., 1985. A mixing-cell solute transport model with exchange of cations in soils. Institute for Land and Water Management Research (ICW), Wageningen, the Netherlands. Nota ICW 1578, 66 p.

HOOGENDOORN, G.H., 1983. Hydrochemie van Oost-Nederland. Deel I-IV. Dienst Grondwaterverkenning TNO, Delft. Rapport nr OS 83-38.

JACKSON, R.E. and R.J. PATTERSON, 1982. Interpretation of pH and Eh trends in a fluvial sand aquifer system. In: Water Resources Research, Vol. 8, No. 4, 1255-1268.

KEMMERS, P.H., 1985. Calcium as hydrochemical characteristic for ecological states. In: Seventh International Symposium on Problems of Landscape Ecological Research, Bratislava.

MOZETO, A.A. et al., 1984. Experimental observations on carbon isotope exchange in carbonate water systems. In: Geochemica et Cosmochimica Acta, Vol. 48, 495-504.

NANCOLLAS, G.H. and M.M. REDDY, 1971. The crystallization of calcium carbonate II: Calcite growth mechanism. In: Journal of Colloid and Interface Science, Vol. 37, No. 4, 824-830.

OMMEN, H.C. VAN, 1985. The mixing-cell concept applied to transport of non-reactive and reactive components in soils and groundwater. In: Journal of Hydrology, Vol. 78, 201-213.

PLESKOV, Y.V. and V.Y. FILINOVSKI, 1976. The rotating disc electrode. Consultant Bureau N.Y., 402 p.

PLUMMER, L.N. et al., 1976. The dissolution of calcite in CO_2-saturated solutions at 25°C and 1 atmosphere total pressure. In: Geochimica et Cosmochimica Acta, Vol. 40, 191-202.

——— et al., 1978. The kinetics of calcite dissolution in CO_2-water systems at 5 to 60°C and 0.0 to 1.0 atm. CO_2. In: American Journal of Science, Vol. 278, 179-216.

——— and W. BACK, 1980. The mass balance approach: applications to interpreting the chemical evolution of hydrologic systems. In: American Journal of Science, vol. 280, 130-142.

RITSEMA, C.J., 1985. Influence of the time on the realization of the $CaCO_3$-equilibrium in soils and on the weathering of feldspars. Institute for Land and Water Management Research (ICW), Wageningen, the Netherlands. Nota ICW 1682, 30 p.

SHUSTER, E.T. and W.B. WHITE, 1972. Seasonal fluctuations in the chemistry of limestone springs: a possible means for characterizing limestone aquifers. In: Journal of Hydrology, Vol. 14, 93-128.

SJOBERG, E.L. and D.T. RICKARD, 1984. Temperature dependence of calcite dissolution kinetics between 1 and 62°C at pH 2.7 to 8.4 in aqueous solutions. In: Geochemica et Cosmochimica Acta, Vol. 48, 485-493.

——— and D.T. RICKARD, 1984. Calcite dissolution kinetics: surface speciation and the origin of the variable pH dependence. In: Chemical Geology, Vol. 42, 119-136.

SOIL SURVEY INSTITUTE OF THE NETHERLANDS, 1965. De bodem van Nederland. Toelichting bij de bodemkaart van Nederland, schaal 1: 200 000.

STUMM, W. and J.J. MORGAN, 1970. Aquatic chemistry.An introduction emphasizing chemical equilibria in natural waters. Wiley-Inter science, New York.

SUAREZ, D.L., 1977. Ion activity products of calcium carbonate in waters below the root zone. In: Soil Science Society of American Journal, Vol. 41, 310-315.

——— and J.D. RHOADES, 1982. The apparent solubility of calcium carbonate in soils. In: Soil Science Society of American Journal, Vol. 46, 716-621.

WIECHERS, H.N.S. et al., 1974. Calcium carbonate crystallization kinetics. In: Water Research, Vol. 9, 835-845.